



Hydrogeological investigation of fluoride ion in groundwater of Ruparail and Banganga basins, Bharatpur district, Rajasthan, India

Vikas Rena¹ · Chandrashekhar Azad Vishwakarma¹ · Priyadarshini Singh¹ · Nidhi Roy¹ · Harshita Asthana¹ · Vikas Kamal¹ · Pardeep Kumar¹ · Saumitra Mukherjee¹

Received: 9 October 2020 / Accepted: 11 July 2022 / Published online: 29 August 2022
© The Author(s), under exclusive licence to Springer-Verlag GmbH Germany, part of Springer Nature 2022

Abstract

Hydrochemical analysis, geological study and evaluation of hydrogeochemical processes play a crucial role to understand the variability of fluoride ion concentration in groundwater. The present study is focused on a watershed boundary comprising of parts of two river basins namely Ruparail and Banganga within Bharatpur district of Rajasthan in India. Administratively, the study area is covered in five blocks of Bharatpur district viz. Deeg, Kaman, Nagar, Pahari and Kumher. The study area and sampling locations were identified based on the spectral signatures of satellite data, literature study and field-based experience. Seventy-five groundwater samples were collected for pre and post-monsoon seasons, separately. The hydrochemical results have shown that Banganga basin has experienced greater fluoride enrichment in groundwater as compared to Ruparail basin. Both the basins have experienced more groundwater samples in the class of high-risk water (more than 1.5 mg/l F⁻) during the post-monsoon season due to mineral dissolution with the surface run-off water in the aquifer material. The shallow aquifers (<40 m bgl) have experienced high fluoride distribution in groundwater as compared to deeper aquifers (>40 m bgl). The spatiotemporal interpolation maps for fluoride ion concentration generated by following inverse distance weighted (IDW) method have shown the varied fluoride concentration with geologic, geomorphic and seismotectonic features. Chadha's plot for hydrochemical facies has revealed that the groundwater of the study area is mainly of Na–Cl and Ca–Mg–Cl type. The evaluation of hydrochemical facies has suggested that Na–Cl water type is having elevated fluoride ion concentration as compared to Ca–Mg–Cl and Ca–Mg–HCO₃ water types. The interpretation of hydrogeochemical processes based on scatter plots of hydrochemical parameters has revealed that processes such as silicate weathering, direct-ion exchange, mineral dissolution and rock–water interaction are responsible for fluoride augmentation in groundwater. The enrichment is also governed by evaporation, semiarid environment, salinity hazard and overdraft of groundwater. The water types having inhibited fluoride ion concentration are found dominated with carbonate weathering and recharge water (Ca–Mg–HCO₃ type) and reverse-ion exchange process (Ca–Mg–Cl type). Moreover, the geochemical modeling is indicative of under-saturation of fluorite with over-saturation of calcite and dolomite, augmenting fluoride ion concentration in groundwater. The comprehensive understanding of hydrogeochemical processes controlling fluoride enrichment is found useful for planning strategies adopted for providing safe drinking water in a sustainable way.

Keywords Hydrochemistry · Hydrogeochemical processes · Fluoride ion · Ruparail basin · Banganga basin · Spatiotemporal variation

This article is part of a Topical Collection in Environmental Earth Sciences on Groundwater quality and contamination and the application of GIS, guest edited by Narsimha Adimalla and Hui Qian.

✉ Saumitra Mukherjee
saumitramukherjee3@gmail.com; saumitra@mail.jnu.ac.in

¹ Remote Sensing Applications Laboratory, School of Environmental Sciences, Jawaharlal Nehru University, New Delhi 110067, India

Introduction

Since the advent of human civilization, life has been and would always prosper in the proximity of water resources (Adimalla et al. 2020b; Priscoli 2000; Yevjevich 1992). Among all the forms of water, groundwater plays a crucial role in domestic, industrial and agricultural demands of water (Hussain and Abed 2019). Fluoride ion concentration in groundwater constraints the groundwater appropriateness

for human consumption (Adimalla et al. 2021; Subramani et al. 2005). The present study pertains to groundwater quality aspect with particular reference to fluoride ion concentration, and the associated geochemical processes responsible for variation in fluoride ion concentration. The variation is also evaluated with the specific lithologic, geomorphic and tectonic features there in the study area.

Fluoride is one of the most critical elements of human health. Fluoride plays a crucial role in bones mineralization and dental-enamel formation in the human body (Chouhan and Flora 2010). However, an excess amount of fluoride causes skeletal as well as non-skeletal fluorosis in the human body (Hussain et al. 2010; Singh et al. 2007). Previous studies have reported that the world is facing fluorosis as a key health issue due to high fluoride in drinking water (Adimalla et al. 2020a; Ayoob and Gupta 2006). The world is facing a major impact on human health from the consumption of drinking water contaminated with iron, followed by fluoride, salinity, nitrate and arsenic (Cotruvo 2017). In India, 63–65 million people have access to water for drinking purposes with higher fluoride concentration as per guidelines of BIS (Athavale and Das 1999; Muralidharan et al. 2002; Rao 2006; Susheela 1999). Rajasthan, being the largest state of India, 342,239 Sq. Km., has 10.41% of the country's geographical area and with 5.5% of the nation's population, but has only 1% of the water resources of India (Saxena and Saxena 2013). At the district level of Rajasthan, many researchers have found out that all the 33 districts of Rajasthan have fluorosis prone areas (Hussain et al. 2012; Singh et al. 2011, 2001). The previous literature indicated that the fluoride contamination of groundwater caused dental fluorosis in the adjacent areas to the study area (Dubey et al. 2015; Tiwari and Mondal 2018). The contaminated sources with fluoride affecting humans and animals are mainly from groundwater, crops grown on fluoride-rich soils and dust from the atmosphere. Nowadays, coal burning and industrial activities also discharge fluoride in gaseous and particulate dust forms (Fuge 2018). The safe limit of fluoride ion in drinking water is 1.5 mg/l and 1.0 mg/l prescribed by World Health Organization (WHO 2017; Cotruvo 2017) and Bureau of Indian Standards (BIS 2015), respectively.

Satellite-based remote sensing in addition to Geographic Information System (GIS) has emerged as an important tool in water resource development and management. However, the satellite-based remote sensing application is still low in hydrology applications since the information provided by the sensors is restricted to a few centimeters below the earth surface only (Bandyopadhyay et al. 2007). Moreover, the GIS environment has a significant role in the spatiotemporal distribution of hydrochemical parameters of groundwater (Mondal et al. 2016). The spatial analyst tool of ArcGIS 10.2 offers various interpolation methods for spatiotemporal evaluation. The interpolation method prepares

a continuous dataset by predicting the values of un-sampled locations from the values of sampled locations. Inverse distance weighted (IDW) and kriging are the two commonly used interpolation methods for characterizing the groundwater quality and interpolating the values where data point lacks (Zandi et al. 2011). IDW as a deterministic method and kriging as a geostatistical method were performed in both spatial and geospatial analyst tool of Arc GIS 10.2. The IDW method is adopted for mapping the fluoride ion concentration in groundwater as it is showing the least root-mean-square error (RMSE) (Kumar et al. 2011).

Statistical evaluation methods such as correlation matrix analysis and principal component analysis (PCA) of hydrochemical parameters give a broad understanding of dominant reactions and hydrochemical processes (Elango et al. 1992; Houria et al. 2020; Kumar et al. 2014; Subba Rao et al. 2020). PCA is a dimensionality reduction multivariate statistical analysis technique used to find out the association between variables through diagonalization of the correlation matrix (Salifu et al. 2012). PCA is applied on a large dataset of variables to extract principal components (PC's), explaining the major part of the information of the original dataset. The eigenvalue is extracted from the covariance matrix of the original dataset based on scree plot, explaining the structure of the data matrix. PC's are the orthogonal (uncorrelated) variables obtained by multiplying the original variables with the eigenvector (loadings) (Mohammadi 2009).

Fluoride in the aqua-chemistry comes from the dissolution of fluoride-bearing minerals (Raju et al. 2009). Fluoride bearing minerals may be fluorite, fluorapatite, biotite, muscovite, hornblende, tremolite and some micas. These minerals dissolved in groundwater as a result of weathering process of igneous and sedimentary rocks and leaching from aquifer sediments through the infiltration of recharge water (Adimalla 2020; Bo et al. 2003; Datta et al. 1996b; Fazelabdolabadi and Golestan 2020; Handa 1975; Singh et al. 2014). Evaporation, crystallization, dilution due to weathering and rock–water interaction are the vital processes controlling fluoride ion concentration in groundwater (Mohapatra et al. 2011; Singh et al. 2018). The amount of precipitation and the rate of evapotranspiration impact the climatic variability of the region and also have a crucial impact on water resource management (Thanh 2019). Overburden on groundwater resources, extensive use of fertilizers and change in land use–land cover are the other significant factors that control groundwater chemistry (Houria et al. 2020; Zaidi et al. 2015). Therefore, the present study aims at the assessment of fluoride contamination in groundwater of Ruparail and Banganga basins of Bharatpur district and the evaluation of associated hydrogeochemical processes for fluoride in groundwater. The varied geologic and geomorphic settings in the two basins along with aquifer depth offer the better

understanding of fluoride concentration in groundwater in accordance with the hydrogeological environment.

Study area

The present study is focused on a part of Bharatpur district of Rajasthan, India (Fig. 1a). It is located on the eastern plains of Rajasthan and situated in the east of Aravalli hill range. Administratively, the district is divided into ten blocks and three subdivisions, i.e., Deeg, Bharatpur and Bayana. There are three hydrological basins within the entire district, namely Rupa rail, Banganga and Gambhiri. The present study area is a delineated watershed boundary covering some watersheds of Rupa rail and Banganga basin, within five blocks, viz. Deeg, Kaman, Nagar, Pahari and Kumher of Bharatpur district (Fig. 1b) and seventy five groundwater sampling points were identified across the study site during premonsoon (Fig. 2c) and postmonsoon (Fig. 2d) seasons. Since both the basins are a part of Yamuna middle sub-basin, the entire study area has a gentle easterly slope toward the river Yamuna. The study area demarcation was carried out by following stream network covering the maximum part of the Deeg subdivision (Fig. 2a). The study area lies between 77°02'40.536" E to 77°24'37.097" E longitude and 27°19'39.359" N to 27°45'15.482" N latitude covering an area of 944.40 km².

All the major rivers (Rupa rail, Banganga and Gambhiri) of the district, originate from outside the district and flow for a quite shorter duration during the monsoon period only. The river Rupa rail is also known as Barah River originates from Thangazi hills of Alwar district of Rajasthan, whereas Banganga River debouches from Aravalli hills near Arnasar and Bairath in Jaipur district of Rajasthan. Since the area has no perennial river, groundwater performs as the primary source of water supply in the locality (Chadha 2006). The present study is focused on a watershed catchment boundary comprising of two adjacent river basins viz. Banganga and Rupa rail river basins within the Bharatpur district of Rajasthan (Fig. 2a).

Rupa rail basin

The Rupa rail river basin is located in the northeastern part of Rajasthan and is bounded by The Sabi river basin in the northwestern side and the Banganga river basin in the southeastern side. A total of 70.7% catchment area of the basin falls in Alwar district of Rajasthan, and the rest (29.3%) falls within the Bharatpur district of Rajasthan. The basin is stretched into Kaman, Pahari, Nagar and Deeg blocks of Bharatpur district in Rajasthan. Rupa rail basin covers 395.70 km² area of the study site.

Banganga basin

Banganga river basin is covered by Bharatpur District (29.48%) followed by Alwar (27.20%), Dausa (24.99%), Jaipur (15.41%), Karauli (2.85%), Sawai Madhopur (0.06%) and Sikar (0.01%) districts of Rajasthan. The basin is stretched into Deeg, Kumher, Nagar, Sewar, Nadbai, Weir, Rupbas and Bayana blocks of Bharatpur district (Vyas et al. 2016; Yadav et al. 2019). Banganga basin covers 548.70 km² area of the study site.

The district has an arid climate with a hot and dry summer and cold winter, while monsoon stays for a shorter period in the study area. The district receives 645.35 mm annual rainfall during 2016 as compared to 557.60 mm of normal rainfall. The district logs 15.7% more rainfall in the year 2016 from the normal precipitation budget. More than 90% of rainfall is contributed by the southwest monsoon in the study area. The study area comprises of 41.90% area under Rupa rail basin and 58.10% area covering Banganga basin. Clay loam and loam soils are most prevalent in the study area. Soil salinity, soil hydraulic properties and alkalinity are the major problems that can be attributed to groundwater salinity and shallow water table in the region (CGWB 2017). Agricultural activity in the area is mainly of Kharif crops depending upon precipitation and Rabi crops depending upon the available irrigation facility.

Variation in the depth to groundwater level depends upon topography, geology, drainage and bedrock. As per Central Groundwater Board (CGWB) report, 2017, the groundwater is found at varying depths in different blocks as Deeg (4.10–14.13 m bgl), Kaman (10.67–12.33 m bgl), Nagar-Pahari (6.98–11.80 mbgl) and Kumher (5.98–11.40 m bgl) (CGWB 2017). In Rupa rail basin, the groundwater of varying depths was collected from 15–90 m bgl during pre-monsoon season and 3–60 m bgl during post-monsoon season. The groundwater was also collected from 10–80 m during pre-monsoon and 5–75 m during post-monsoon season in Banganga basin. The shallow aquifers are characterized as less than 40 m bgl, whereas deep aquifers as more than 40 m bgl. The previous literature suggest the augmented fluoride ion concentration in shallow aquifers having weathered soil and clay material as compared to deep aquifers having fractured hard rock terrain (Vikas et al. 2013). Table 1 explains the fluoride distribution in groundwater of shallow and deep aquifers during pre- and post-monsoon season.

Hydrogeology

The study area has a distinct type of geology which is tectonically, lithologically and structurally very rich and mainly of Delhi supergroup as shown in Fig. 2b. The Delhi supergroup rocks are classified into Alwar and Ajabgarh group

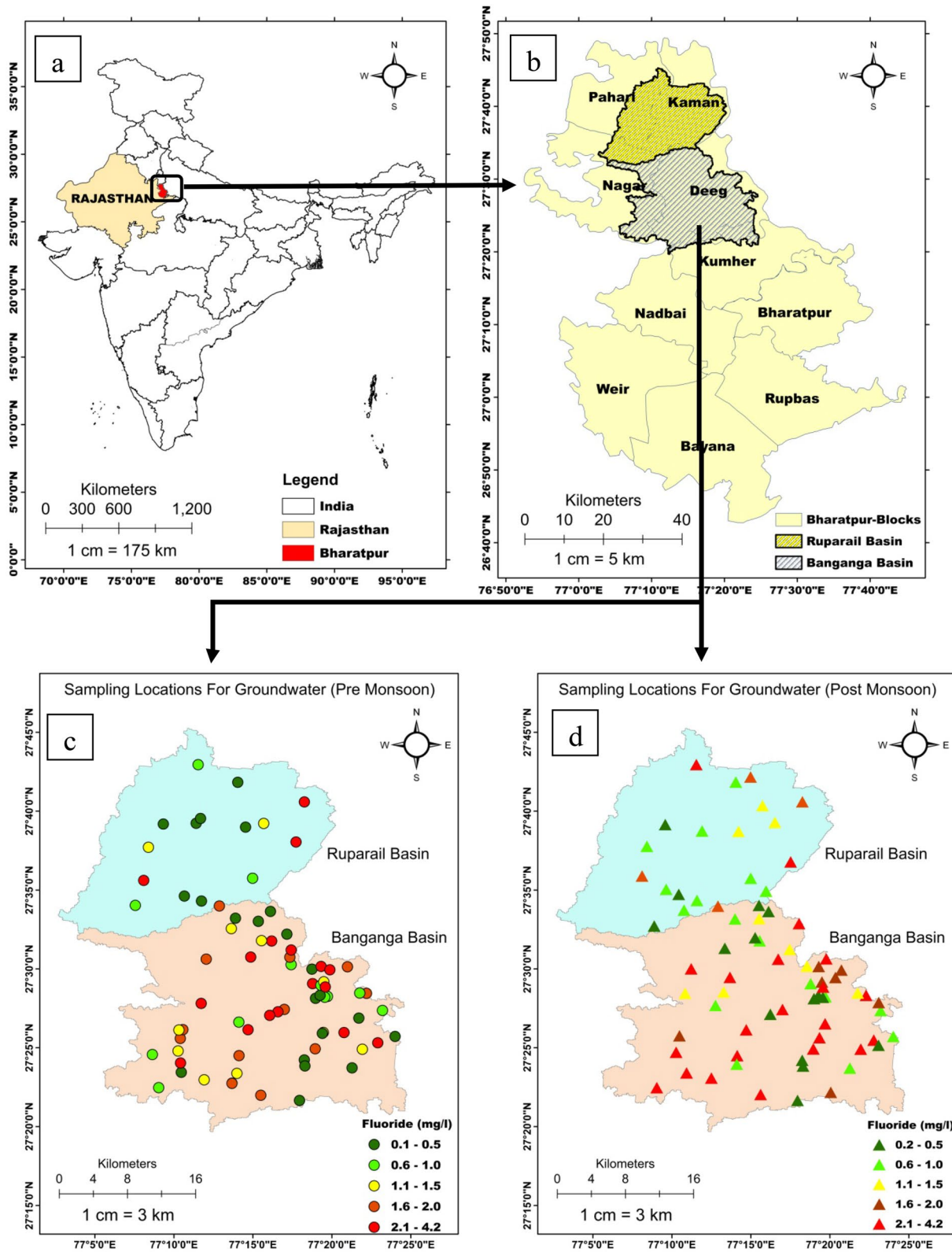


Fig. 1 Study area map showing location within **a** India, **b** Comprising Ruparail and Banganga basins within Bharatpur district administrative boundary and groundwater sampling location with fluoride ion concentration for **c** Pre-monsoon and **d** Post-monsoon seasons

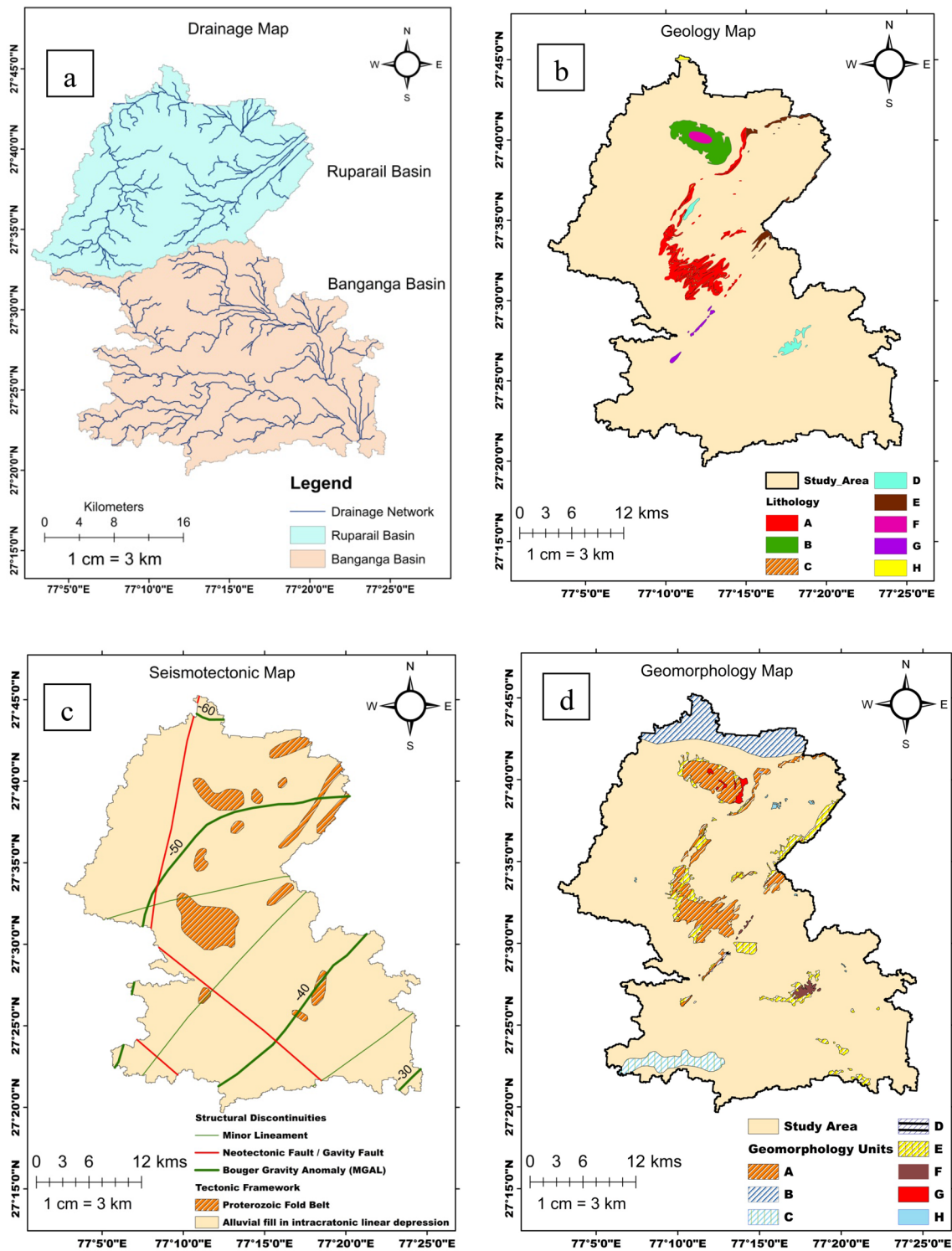


Fig. 2 a Watershed drainage map b Geology map, where A: Phyllite interbedded with quartzite; B: Orthoquartzite; C: Quartzite; D: Carb. phyllite, shale, slate, intercalated Qtz; E: Interbedded quartzite, schist and phyllite; F: Massive Qtz. locally feldspathic and gritty Sst; G: Quartzite with phyllite and schist; H: Oxidized silt-clay with kankar And micaceous sand. c Seismotectonic map d Geomorphology map (Din and Javed, 1997; NRSC 2012), where A: Structural origin_mod-

erately dissected hills and valleys; B: Denudational origin moderately dissected hills and valleys; C: Denudational origin pediment plain; D: Fluvial origin younger alluvial plain; E: Fluvial origin older alluvial plain; F: Fluvial origin_older flood plain; G: Anthropogenic origin_anthropogenic terrain; H: Water bodies_ponds; I: Study area

Table 1 Depth-wise classification of fluoride contamination in groundwater

Water class	Fluoride ion concentration	Pre-monsoon		Post-monsoon	
		Shallow aquifer (< 40 m bgl)	Deep aquifer (> 40 m bgl)	Shallow aquifer (< 40 m bgl)	Deep aquifer (> 40 m bgl)
Safe	< 0.50 mg/l	30.56	54.55	12	50
Low risk	0.50–1.50 mg/l	27.78	27.27	36	25
High risk	> 1.50 mg/l	41.67	18.18	52	25

* mbgl meters below ground level

formations. Alwar group has Pratapgarh type, whereas Ajabgarh group has Bhakrol and Arauli types of stratigraphy. The geology is mainly of Paleoproterozoic/Mesoproterozoic period of formation. Undifferentiated fluvial and aeolian sediment covers maximum part of the southern region in the study area. The northern part of the study area is covered by Lalsot hills and Kaman-Pahari isolated hills, which are distal exposure of isolated hills from Ajabgarh sedimentation of Delhi supergroup formation. The quartzite interbedded with schist and phyllite has been assigned to Bhakrol formation of Ajabgarh group. Domal outcrop of feldspathic sandstone and orthoquartzite exposed between Pahari and Kaman has been assigned to Pratapgarh formation of Alwar group (CGWB 2017). In the central region of the study area, Ajabgarh group metasediments are most prevalent. These have a predominance of Argillaceous rocks and consist mainly of phyllite, slate, impure limestone and quartzites. The major part of the study area is covered by alluvium of varying thickness and comprising of sand, silt, clay and kankars. The deepest occurrence of bedrock indicating high alluvium deposits of 100–140 m bgl (Below Ground Level) is found in Kaman and Pahari blocks of Ruparail basin. Deeg, Nagar and Kumher blocks within Banganga basin having moderately deep bedrock overlain by low alluvial thickness are found to be at 60–100 m bgl. The groundwater flow can be generalized as SW to NE. Hydraulic gradient in the study area was observed as 0.86 m/km (Chadha 2006). The significant part of the study area is under Older Alluvium (Quaternary) deposits. Previous study explains the discharge rate as 150–450 m³/day from Tube wells and Dug cum borewells (Chadha 2006).

Seismotectonic features

There are four major types of seismotectonic features within the study area viz., Proterozoic fold belt, Bouguer gravity anomaly, Neotectonic fault/gravity fault and minor lineaments as shown in Fig. 2c. The features were identified with the help of remote sensing data (RapidEye 2 satellite imagery-5 m and SRTM-30 m), Seismotectonic Atlas of India (Survey of India) and ArcGIS 10.2. Proterozoic fold belt is mainly represented by the Delhi group and is the

main structural grain of this area. There are several faults/lineaments traverse along with this trend. Among these most conspicuous one is the Great Boundary Fault trending in the NE–SW direction between Archeans (Delhi supergroup) and Vindhyan. The isolated gaps are due to wrench tectonics within the study area. Bouguer gravity anomaly contours display a general pattern following the main tectonic grain. Toward the south, the gravity value gradually decreases up to Bharatpur-Mt. Abu Lineament. Earthquakes from historical and pre-industrial period lie near the Yamuna river course between Delhi and Mathura. Neotectonic fault/gravity fault and minor lineaments are found as structural discontinuities within the study area.

Geomorphology

The earth observation datasets (RapidEye 2 satellite imagery-5 m and SRTM-30 m) in conjunction with SOI Toposheets and Bhukosh geoscientific dataset were used to prepare a geomorphological map of the study area as shown in Fig. 2d. The landform features across the study area were classified into three levels of the geomorphological classification system (NRSC 2012). Genesis-based geomorphology of fluvial, denudational, structural and anthropogenic origin types covering an area of 137.17 km² is prevalent in the study area. A total of seven types of geomorphic features are found in an order of structural origin (SO)—moderately dissected hills and valleys (47 km²), fluvial origin (FO)—older alluvial plain (41 km²), denudational origin (DO)—pediment plain (29 km²), FO—younger alluvial plain (15 km²), DO—moderately dissected hills and valleys (3 km²), anthropogenic origin (AO)—anthropogenic terrain (2 km²) and FO—older flood plain (0.53 km²) across the study site. In addition to this, Hog-back ridge, Cuesta, Loess and erosional depressions are also peculiar features in the study area. FO alluvial plains are formed as an undulating terrain consisting of gravel, clay, silt, sand and gravels. FO flood plains are explained as relatively smooth land surface adjacent to a channel and subjected to periodic flooding. SO valleys are formations crossed by fractures forming deep valleys, whereas SO hills are linear to curved hills with

folds. DO dissected hills and valleys comprise of anomalous lithology and joints, fractures and lineaments (CGWB 2017; Din and Javed 1997).

Materials and methods

The study area comprising of Ruparail and Banganga hydrological basins was delineated with the help of watershed hydrological transport model SWAT (Soil and Water Assessment Tool) by using SRTM (Shuttle Radar Topography Mission-30 m resolution) dataset. The sampling locations for groundwater and sediment (rock and soil) were marked based on varied spectral responses of various features using remotely sensed data (SRTM-30 m and RapidEye View2 satellite imagery-5 m), detailed literature study and field-based experience. Seventy-five locations for groundwater and forty locations for sediments (rock and soil) were identified across the study area. The groundwater samples were collected for two seasons, i.e., pre-monsoon and post-monsoon for a comprehensive assessment of seasonal change in hydrochemistry. The geo-coordinates for the sampling locations were marked by using Garmin Global Positioning System (GPS). The groundwater samples were collected from dug-well, tube-well and hand-pumps. To avoid iron pipe contamination, 10–20 strokes of hand-pump were spilled out without collecting the sample. After that, groundwater samples were collected in acid-washed high-density polypropylene plastic bottles (TARSON) of two sizes, 125 ml and 250 ml. At the time of sample collection, the bottles were rinsed properly with the sample, and the groundwater was filled up to brim with utmost care to avoid any contamination and oxidization of the water sample. After the collection of groundwater in a 125 ml sampling bottle, a few drops of concentrated HNO_3 (Nitric acid) were added to stabilize the heavy metals for further analysis (American Public Health Association 1995; Singh et al. 2014, 2018). Some of the physicochemical parameters were analyzed on the site with handheld instruments. Temperature, pH, electrical conductivity (EC), total dissolved solids (TDS) and salinity were analyzed by using Thermo Fisher multi-parameter TESTR 35 series. Alkalinity was also analyzed using Aquamerck Kit for alkalinity test. Further, major cations and anions were analyzed in the laboratory by using laboratory-based experiments. The anions such as CO_3^{2-} , HCO_3^- and Cl^- were analyzed by using the titrimetric method (American Public Health Association 1995). NO_3^- (TRI method), PO_4^{3-} (Malachite green method), SO_4^{2-} (Barium sulfate method) and F^- (SPANDS method) anions were analyzed based on spectro-photometric analysis by using UV/VIS spectrometer (PerkinElmer-Lambda 35) (American Public Health Association 1995; Diatloff and Rengel 2001). Among major cations, Na^+ , K^+ and Ca^{+2} were analyzed by a flame photometer

(ELICO-CL378), and Mg was analyzed by using atomic absorption spectrophotometer (Thermo Fisher Scientific). The heavy metals present in groundwater were also analyzed by using ICP-OES (Agilent 5110) (American Public Health Association 1995). In general, the ion balance error of the samples was observed in a range of ± 0.05 .

Watershed delineation, drainage network and various thematic maps such as geology, geomorphology and seismotectonic were prepared based on earth observation datasets and Geographic Information System (GIS) environment. SRTM-30 m data were used to prepare SWAT model for watershed delineation, and drainage network was prepared by using the hydrology tool of ArcGIS 10.2. The thematic maps were prepared with the help of Survey of India (SOI) toposheets, geoscientific data from Bhukosh of Geological Survey of India (GSI) and high-resolution satellite data of RapidEye View2 (5 m) using ArcGIS10.2. The image segmentation method was used to prepare the thematic maps of various features using SAGA GIS 2.0.8. The spatiotemporal distribution of fluoride ion in groundwater of the study area was prepared by IDW method of interpolation by using the spatial analyst tool of ArcGIS 10.2.

The Chadha's plot and various scatter plots to understand the hydrochemical facies and geochemical process were prepared by using Microsoft Excel 2010. The detailed study of hydrochemical facies was carried out by using Rockware Aq.QA version 1.1.1 (1.1.5.1). Further, the statistical technique of correlation matrix analysis was carried out using 'R' software version 3.6.3, whereas the principal component analysis was performed on SPSS 16.0. PCA was applied on 20 hydrochemical parameters for 76 water samples during pre-monsoon and 74 during post-monsoon samples following the Varimax method of rotation with Kaiser normalization. According to the criteria of Cattell and Jaspers (1967) and Kaiser (1960), the components with eigenvalues > 1 were retained as principal components. The geochemical modeling for the mineral phase was carried out using USGS geochemical code PHREEQC 3.1.2.

Results

Hydrochemistry

The statistical summary of the results of the hydrochemical analysis of groundwater samples during pre- and post-monsoon seasons within Ruparail and Banganga basins is presented in Table 2 and 3, respectively. Both the basins having elevated electrical conductivity (EC) confirm the major salinity problem within the study area. As compared to Ruparail basin, the Banganga basin is facing severe salinity problem. The elevated EC during post-monsoon in comparison with pre-monsoon season gives a clear indication

Table 2 Statistical summary of groundwater quality parameters during pre- and post-monsoon seasons within the Ruparail river basin of the study area

Parameters	Pre-monsoon				Post-monsoon			
	Min	Max	Average	Std. Dev	Min	Max	Average	Std. Dev
pH	6.30	7.70	7.21	0.37	6.50	7.80	7.13	0.32
EC	257.56	2862.45	1441.65	912.00	534.00	8510.00	3353.20	2413.69
TDS	190.00	2065.00	1042.31	656.46	393.00	6250.00	2417.85	1746.09
Salinity	120.31	1412.39	655.35	471.69	250.00	4500.00	1684.25	1272.21
Alkalinity	140.35	799.36	495.02	191.76	134.24	1025.14	516.23	248.01
Total hardness	140.00	1630.00	515.00	436.33	130.00	3490.00	838.00	819.68
CO ₃ ⁻²	8.07	45.98	28.47	11.03	7.72	58.97	29.69	14.27
HCO ₃ ⁻	134.20	652.70	386.97	157.34	73.20	805.20	332.45	175.24
PO ₄ ⁻³	0.58	1.30	0.76	0.19	0.55	1.53	0.78	0.28
SO ₄ ⁻²	4.32	226.06	103.36	78.94	2.23	198.18	104.21	69.33
F ⁻	0.09	3.80	1.13	1.17	0.11	2.12	1.09	0.63
NO ₃ ⁻	18.57	325.78	77.42	73.78	19.87	189.92	55.24	45.00
Cl ⁻	70.90	2127.34	585.89	560.71	106.68	3491.97	976.61	880.67
Na ⁺	26.40	1183.01	355.23	352.12	27.30	1080.01	409.42	366.27
K ⁺	0.18	18.03	4.54	4.94	0.15	41.82	7.65	11.07
Ca ⁺²	33.10	235.20	122.48	67.03	32.50	929.70	181.77	194.91
Mg ⁺²	13.33	258.23	81.54	63.59	21.83	441.96	135.97	112.67
Fe	ND	4.25	1.24	1.18	ND	2.82	0.50	0.73
Zn	ND	3.19	0.55	0.87	ND	1.78	0.29	0.52
Sr	0.15	3.05	1.54	1.14	0.17	3.00	1.51	1.07

* All values are in mg/l except pH and EC

pH No unit, EC (Electrical Conductivity) μ S/cm, Min. Minimum, Max. Maximum, Avg. Average, Std. Dev. Standard Deviation, ND Not detected

that the minerals are getting weathered and leaching from aquifer sediments through the infiltration of recharge water or precipitation (Rena et al. 2021). In Ruparail and Banganga basins, the dominant anions follow the same order of $\text{Cl}^- > \text{HCO}_3^- > \text{SO}_4^{-2} > \text{NO}_3^- > \text{CO}_3^{-2} > \text{F}^- > \text{PO}_4^{-3}$ in groundwater during both seasons. The major cations in the groundwater of the two basins are found in the dominance order of $\text{Na}^+ > \text{Ca}^{+2} > \text{Mg}^{+2} > \text{K}^+$ during both seasons. These dominance orders are suggestive of silicate weathering and the direct-ion exchange process in the region (Singh et al. 2011, 2018). Fe, Sr and Zn are the three major heavy metals found in the groundwater chemistry of the study area. The heavy metals are found in the dominance order of $\text{Sr} > \text{Fe} > \text{Zn}$ during both seasons in Ruparail basin, whereas in the order of $\text{Fe} > \text{Sr} > \text{Zn}$ during both season in Banganga basin. The ionic concentration of various elements in groundwater is further used for better understanding of dominant hydrochemical processes and mechanisms in the two basins during both seasons.

Fluoride distribution and contamination in groundwater

The concentration of fluoride ion in groundwater samples of Ruparail basins was found in the range of 0.09 mg/l–3.80 mg/l

(average 1.13 mg/l) during pre-monsoon, whereas it ranged from 0.11 mg/l to 2.12 mg/l (average 1.09 mg/l) during post-monsoon season. The Banganga basin has experienced the fluoride ion concentration in groundwater ranged from 0.09 mg/l to 4.23 mg/l (average 1.37 mg/l) during pre-monsoon, whereas it ranged from 0.15 mg/l to 4.19 mg/l (average 1.50 mg/l) during post-monsoon season. The fluoride ion concentration in groundwater samples was found above the permissible limit of drinking water of 1.5 mg/l, (World Health Organization 2017; Cotruvo 2017) in 25 and 30% during pre and post-monsoon seasons, respectively, in Ruparail basin, whereas 41.67 and 50% during pre- and post-monsoon season, respectively, in Banganga basin. As per the guidelines of drinking water prescribed by Bureau of Indian Standards (BIS), of 1 mg/l (Bureau of Indian Standards 2015), 37.50 and 45% during pre and post-monsoon seasons, respectively, in Ruparail basin, whereas 56.67 and 61.11% during pre and post-monsoon seasons, respectively, in Banganga basin.

The spatial distribution of fluoride ion concentration in groundwater during pre- and post-monsoon seasons is shown in Fig. 3a, b comprising of both the basins. The spatial distribution maps were prepared by following the IDW (inverse distance weighted) method of interpolation using the Spatial Analyst Tool of ArcGIS 10.2. In the pre-monsoon season, Fig. 3a, the greater fluoride ion concentration is found in

Table 3 Statistical summary of groundwater quality parameters during pre- and post-monsoon seasons within the Banganga river basin of the study area

Parameters	Pre-monsoon				Post-monsoon			
	Min	Max	Average	Std. Dev	Min	Max	Average	Std. Dev
pH	6.40	8.80	7.30	0.39	6.50	8.00	7.29	0.34
EC (μS)	507.63	5620.16	2237.23	907.41	849.00	15,430.00	4435.18	3310.72
TDS	370.00	4050.00	1614.97	653.15	560.00	10,700.00	3196.35	2383.68
Salinity	238.02	2930.91	1070.15	495.95	405.00	9200.00	2274.05	1855.69
Alkalinity	61.02	1263.11	617.52	274.93	152.55	1757.38	601.05	316.80
Total Hardness	20.00	9410.00	1266.33	1609.47	80.00	5410.00	1099.81	1216.37
CO_3^{-2}	3.51	72.66	35.52	15.81	8.78	101.09	34.57	18.22
HCO_3^{-}	152.50	1067.45	500.90	239.32	48.78	1165.10	368.19	221.70
PO_4^{-3}	0.55	2.58	0.87	0.40	0.53	1.58	0.77	0.21
SO_4^{-2}	27.05	270.73	155.26	57.81	24.00	282.42	119.99	51.00
F^{-}	0.09	4.23	1.37	1.06	0.15	4.19	1.50	0.94
NO_3^{-}	12.51	237.09	47.12	36.80	13.78	192.08	45.50	33.68
Cl^{-}	141.80	14,586.75	1889.27	2360.25	141.75	8685.25	1728.33	1875.20
Na^{+}	38.50	4565.99	917.28	847.76	42.68	3618.00	779.85	804.76
K^{+}	1.08	443.20	40.68	91.52	0.37	403.46	31.46	71.07
Ca^{+2}	34.10	1110.00	255.20	190.28	59.10	712.50	250.94	154.29
Mg^{+2}	1.21	1503.16	211.82	271.83	7.29	925.21	176.76	207.45
Fe	ND	39.41	3.16	6.77	ND	17.24	2.23	3.91
Zn	ND	3.24	0.36	0.69	ND	3.16	0.33	0.58
Sr	0.24	3.00	2.21	0.97	ND	3.18	1.97	1.03

*All values are in mg/l except pH and EC

pH No unit, *EC* (Electrical Conductivity) $\mu\text{S}/\text{cm}$, *Min.* Minimum, *Max.* Maximum, *Avg.* Average, *Std. Dev.* Standard Deviation, *ND* Not detected

Deeg block within Banganga basin and Kaman block within Ruparail basin as compared to Nagar block in Banganga basin and Pahari block in Ruparail basin. During the post-monsoon season, Fig. 3b, the Nagar block of Banganga basin has experienced the maximum fluoride enrichment within the study area, whereas the overall fluoride ion concentration was higher in the Banganga basin as compared to Ruparail basin. Figure 3a and b shows that Deeg block within Banganga basin has experienced more fluoride enrichment in groundwater as compared to Kaman block within Ruparail basin. The results are also validated with the box-plot explaining the basin-wise variation in fluoride ion concentration during pre- and post-monsoon seasons (Fig. 3c, d).

Fluoride enrichment in groundwater leads to skeletal and non-skeletal fluorosis. Patches on the dental enamel, mottling of teeth and skeletal deformation are the common problems due to the drinking of fluoride-contaminated groundwater (Agrawal et al. 1997; Dubey et al. 2015). Fluoride intake of 0.2–0.5 mg/l daily is necessary for human health, and groundwater is the prime source to fulfill the demand of fluoride ion for human health (Adimalla et al. 2018; Boyle and Chagnon 1995; Jin et al. 2000). If fluoride intake is below 0.5 mg/l, it may create some problems like lack of bone mineralization and dental caries (Mondal et al. 2014). When fluoride intake is between 0.5 and 1.5 mg/l, it may

also cause some patches on the dental enamel (Kharb and Susheela 1994). When fluoride intake exceeds 1.5 mg/l for a longer duration, it causes fluorosis, dental mottling and skeletal deformation. The fluoride concentration of more than 3 mg/l for a long term may cause muscle fiber degeneration, reduced immunity, blood cell deformation and urinary tract-related problems (Maheshwari 2006). Based on various health effects of varied fluoride ion concentration, the groundwater of the region has been classified among three different classes for pre and post-monsoon seasons. Table 4 summarizes groundwater classification based on fluoride ion concentration within the study area.

Genesis of high- and low-fluoride groundwater within seismotectonic and geomorphic features

The genesis of high and low fluoride in groundwater in accordance with the seismotectonic features within the study area as shown in Fig. 2c is studied with the spatial distribution of fluoride during pre and post-monsoon season as shown in Fig. 3a, b. It has been observed that the locations adjacent to Proterozoic fold belts and Bouguer gravity anomaly structures have lesser fluoride enrichment in groundwater. Neotectonic faults have shown a varied combination of higher and lower fluoride concentration

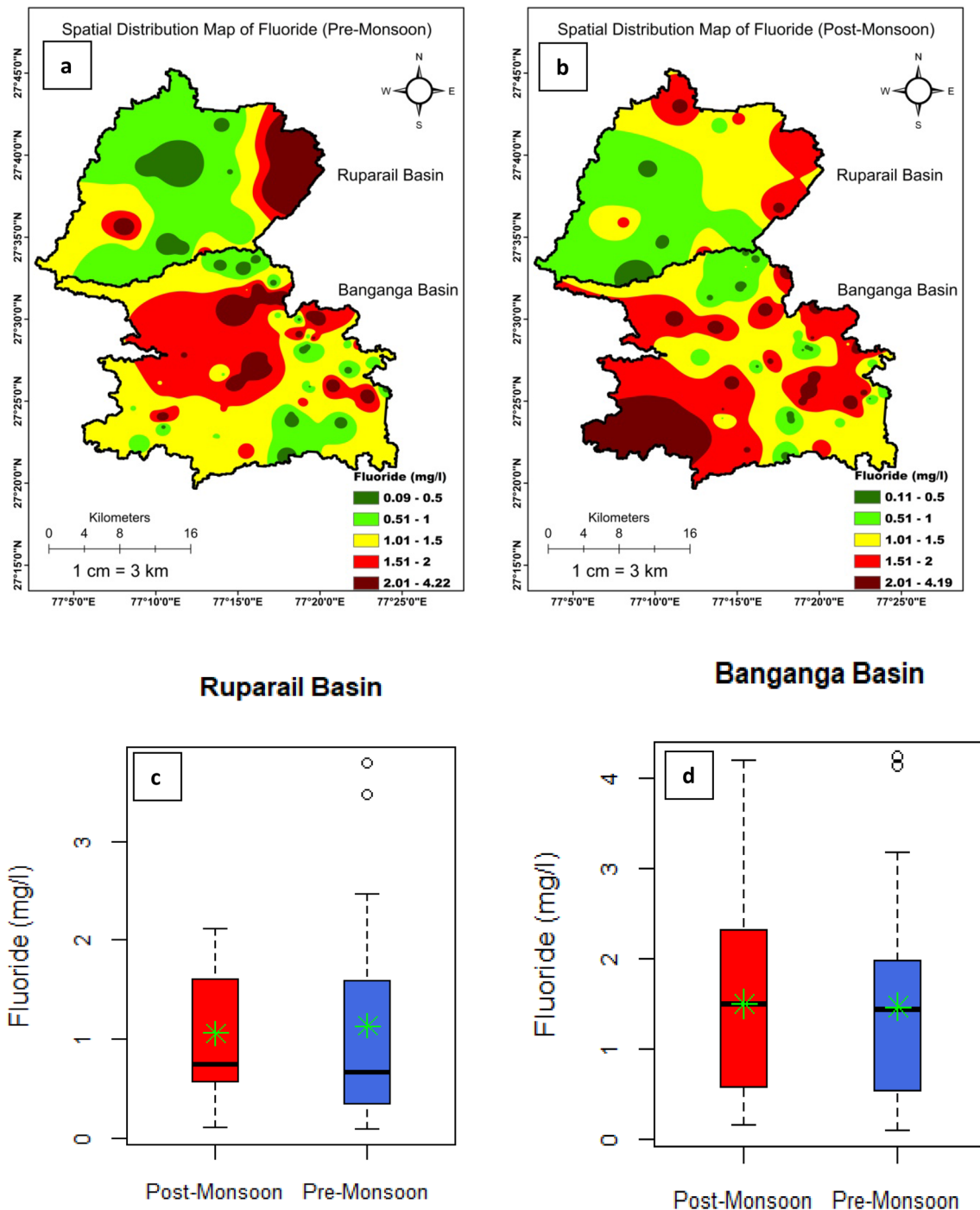


Fig. 3 Spatial distribution of fluoride ion in groundwater during **a** Pre-monsoon, **b** Post-monsoon seasons and fluoride ion concentration boxplot with the mean (star) and median (line) values within **c** Ruparail basin and **d** Banganga basin

based on the adjacent local geomorphic features. Intersection of Neotectonic fault with minor lineament has shown increased fluoride ion concentration during pre-monsoon as compared to post-monsoon. Such intersection, when found near to 'Fluvial origin-Younger alluvial plain,' shows lesser fluoride concentration during pre-monsoon

and higher level during post-monsoon. So, tectonic structure of Proterozoic fold belt has shown lesser fluoride ion concentration, whereas Neotectonic fault and minor lineaments have expressed varied fluoride ion concentration. Along with tectonic features, geomorphic structures have

Table 4 Classification of Groundwater samples based on fluoride ion concentration in Ruparail and Banganga river basins during pre and post-monsoon seasons

Water Class	Fluoride ion concentration	Ruparail basin		Banganga basin	
		Pre-monsoon	Post-monsoon	Pre-monsoon	Post-monsoon
Safe	<0.50 mg/l	43.8	15	28.3	22.2
Low risk	0.50–1.50 mg/l	31.2	55	30	27.8
High risk	> 1.50 mg/l	25	30	41.7	50

*All values are in percentage

Table 5 Hydrochemical facies of groundwater samples using Chadha’s plot in Ruparail and Banganga basins during pre and post-monsoon seasons

Hydrochemical facies	Ruparail Basin		Banganga Basin	
	Pre-monsoon	Post-monsoon	Pre-monsoon	Post-monsoon
Na–Cl type	43.75	35	58.33	50
Ca–Mg–Cl type (reverse-ion exchange water)	31.25	55	33.33	48.15
Ca–Mg–HCO ₃ type (recharge water)	25	10	3.33	0
Na–HCO ₃ type	0	0	5	1.85

* All values are in percentage

also imparted a significant contribution in fluoride ion concentration in the hydrogeologic environment.

The genesis of fluoride in groundwater has been studied with the geomorphology units within the study area as shown in Fig. 2d, and the spatial distribution of fluoride during pre- and post-monsoon season is shown in Fig. 3a, b. It is found that the fluvial origin of the older alluvial plain has shown higher fluoride concentration (up to 4.13 mg/l) in pre-monsoon season, whereas younger alluvial plain has shown fluoride enrichment (up to 4.19 mg/l) in the post-monsoon season. A sharp decline in fluoride ion concentration (up to 0.09 mg/l) is observed in types of landform features of ‘Structural origin—moderately dissected hills and valleys’ and ‘Denudational origin—pediment pediplain complex.’ The ‘Denudational origin—moderately dissected hills and valleys’ and ‘Fluvial origin—older floodplains’ were fluoride-enriched in both pre- and post-monsoon seasons. In contrast to this, ‘Denudational origin—pediment pediplain complex’ has observed both higher and lower concentrations of fluoride, depending upon the adjacent landform features. So, the inhibited fluoride ion concentration was observed in the ‘structural origin—moderately dissected hills and valleys’ and ‘denudational origin—pediment pediplain complex’ type of landform features, whereas ‘fluvial origin—older alluvial plain’ and ‘younger alluvial plain’ landform features have shown augmented fluoride ion concentration. The geochemical modeling of mineral phases is suggestive of the presence of carbonate minerals (calcite, dolomite and aragonite), sulfate mineral (anhydrite and gypsum), iron minerals (hematite and magnetite), manganese mineral (hausmannite), fluorite and halite minerals in groundwater. The groundwater showing under saturated fluorite mineral

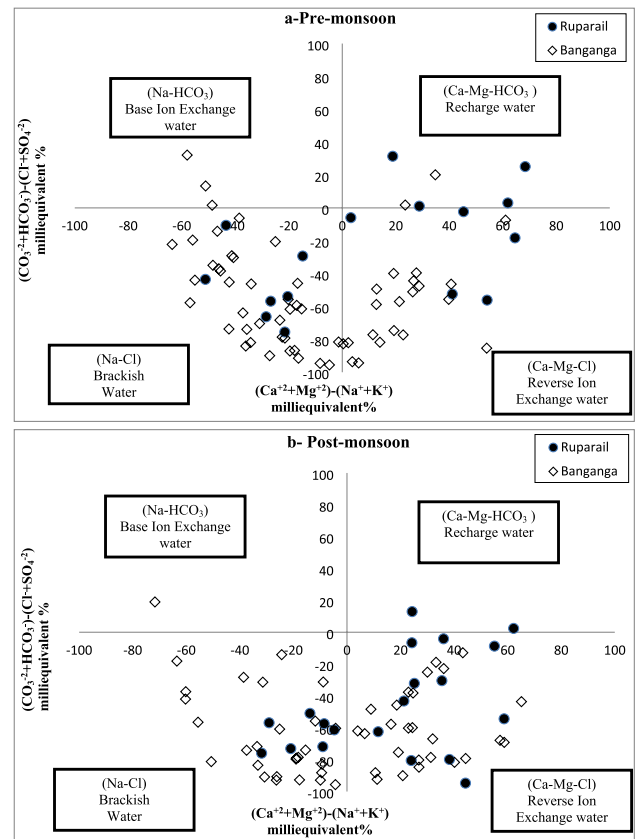


Fig. 4 Chadha plot showing major geochemical processes for groundwater character (Chadha, 1999) during a Pre-monsoon and b Post-monsoon season

phase favors the continual release of fluoride ion from fluorite mineral of aquifer matrices.

Distribution of fluoride ion in groundwater with shallow and deep aquifers

Groundwater depth plays a crucial role in the contamination of fluoride ion in groundwater. The shallow aquifers (< 40 m bgl) have shown an augmented fluoride ion concentration in groundwater as compared to deep aquifers (> 40 m bgl). The high-risk fluoride ion concentration (> 1.50 mg/l) was found to be in shallow aquifers, whereas the deep aquifers have shown more samples with safe fluoride ion concentration (< 0.50 mg/l) as shown in Table 1.

Discussion

Hydrochemical facies

Chadha diagram explains the water type, hydrochemical facies and dominant hydrochemical processes based on water quality parameters. The diagram is plotted by using the difference between alkaline earth (Ca^{+2} and Mg^{+2}) and alkali metals (Na^{+} and K^{+}) in milli-equivalent percentage terms on X-axis. The Y-axis of the diagram is represented by the difference between weak acidic anions (CO_3^{-2} and HCO_3^{-}) and strong acidic anions (Cl^{-} and SO_4^{-2}) in milli-equivalent percentage terms. The Chadha diagram is used to identify four major water types and their associated hydrochemical processes. Figure 4a, b in conjunction with Table 5 is shown that the majority of water samples during both seasons and for both the basins are of Na–Cl type, except during post-monsoon season in the Ruparail basin. The water samples showing Na–Cl water type are the ones in which, alkali metals (Na^{+} and K^{+}) exceed alkaline earth (Ca^{+2} and Mg^{+2}) and strong acidic anions (Cl^{-} and SO_4^{-2}) exceed weak acidic anions (CO_3^{-2} and HCO_3^{-}). The Na–Cl water type can explain the greater salinity hazard within the study area and is associated with the dominant silicate weathering process. The Na–Cl water-type samples are also having higher fluoride ion concentration which can validate

the dominant silicate weathering process responsible for fluoride enrichment. Figure 4a, b shows the second most common water type within the study area is of Ca–Mg–Cl type in which, alkaline earth (Ca^{+2} and Mg^{+2}) exceeds alkali metals (Na^{+} and K^{+}) and strong acidic anions (Cl^{-} and SO_4^{-2}) exceed weak acidic anions (CO_3^{-2} and HCO_3^{-}). The Ca–Mg–Cl type of water is attributed to permanent hardness and no deposition of residual sodium carbonate in irrigation (Chadha 1999). An increase in the percentage of Ca–Mg–Cl type of water samples during post-monsoon season as shown in Table 5 validates the reverse-ion exchange process during post-monsoon season. Table 5 also explains the percentage of groundwater samples showing different hydrochemical facies during pre- and post-monsoon seasons for Ruparail and Banganga basins within the study area. The Ca–Mg– HCO_3 water type explains the recharging water with temporary hardness, whereas the Na– HCO_3 water type is resulted from the dominant base-ion exchange process (Ravikumar and Somashekar 2017).

In order to further validate the hydrochemical facies and water type derived from the Chadha diagram, Aq.QA [1.1.5.1] Rockware tool is used. There were six water types (Na–Cl, Ca–Cl, Mg–Cl, Na– HCO_3 , Mg– HCO_3 and Ca– HCO_3) during pre-monsoon and four water types (Na–Cl, Ca–Cl, Mg–Cl and Na– HCO_3) during post-monsoon identified (Table 6). During both seasons and for both the basins, Na–Cl water type is found dominant followed by Ca–Cl and Mg–Cl. As discussed from the Chadha diagram the water samples from Ruparail basin during post-monsoon season have experienced Mg–Cl water type as compared to Ca–Cl type. Mg– HCO_3 and Ca– HCO_3 water types are found only in pre-monsoon season for a very few water samples, 2 and 1, respectively (Table 6).

Statistical analysis

Statistical methods such as correlation matrix analysis and principal component analysis are used to evaluate the degree of association between different hydrochemical parameters and to extract factors explaining the total variance of the dataset, respectively. In the present study, correlation matrix analysis results are generated using 'R' software version

Table 6 Detailed results of water type of groundwater samples in Ruparail and Banganga basins during pre- and post-monsoon seasons (all values are in percentage)

Water type	Ruparail basin		Banganga basin	
	Pre-monsoon	Post-monsoon	Pre-monsoon	Post-monsoon
Na–Cl type	50	55	75	70.37
Ca–Cl type	18.75	15	11.67	16.67
Mg–Cl type	12.5	25	6.67	11.11
Na– HCO_3 type	6.25	5	5	1.85
Mg– HCO_3 type	12.5	0	0	0
Ca– HCO_3 type	0	0	1.66	0

3.6.3 as shown in Fig. 5. The figure is a tabular form showing the distribution of each variable on the diagonal and the bivariate scatter plot with a fitted line on the bottom of the diagonal. The top of the diagonal explains the value of

the correlation for overall hydrochemical species with the values for pre and post-monsoon seasons, separately. The present analysis depicts the correlation values (r) ranging between + 1 and - 1, where + 1, - 1 and 0 are associated

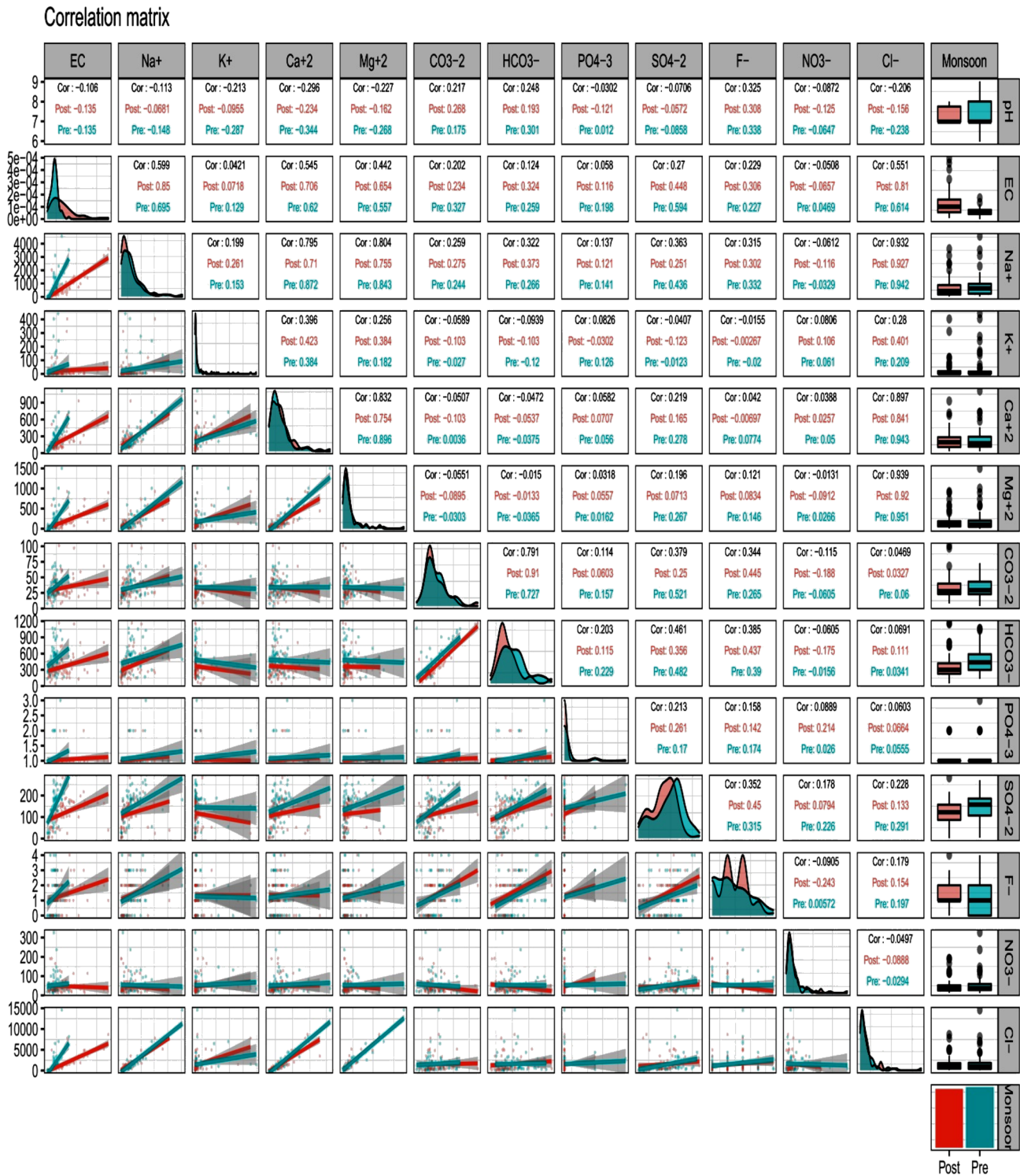


Fig. 5 Correlation matrix analysis for physicochemical parameters of groundwater during pre- and post-monsoon seasons

with perfectly positive linear correlation, perfectly negative linear correlation and no linear correlation between two variables, respectively. According to Adams, the strong, moderate and weak positive correlations were represented by the correlation coefficient ranging from 0.70 to 1.00, from 0.30 to 0.70 and from 0.00 to 0.30, respectively. Similarly, strong, moderate and weak negative correlations were represented by the correlation coefficient ranging from -0.70 to -1.00 , from -0.30 to -0.70 and from 0.00 to -0.30 , respectively (Adams et al. 2001). The figure (Fig. 5) has shown a positive correlation of fluoride with pH (0.325), CO_3^{2-} (0.344) and HCO_3^- (0.385) suggestive of enrichment of fluoride ion in alkaline environment. The positive correlation with EC (0.229) supports the rock–water interaction process and SO_4^{2-} (0.352) supports the silicate weathering process responsible for fluoride enrichment in groundwater (Rina et al. 2013). The fluoride has shown positive correlation (0.315) with Na^+ confirming the fluoride enrichment in Na-Cl type of water. The figure has also shown a negative correlation of fluoride with K^+ (-0.0155) and NO_3^- (-0.0905).

Principal component analysis

PCA was performed on SPSS 16.0 and applied to groundwater quality parameters dataset of pre-monsoon and post-monsoon, to extract principal components defining the sources of variation in hydrochemistry at aquifer level. Before carrying out PCA, the Kaiser–Meyer–Olkin (KMO) Bartlett's sphericity tests were performed in order to examine validity of PCA. KMO test value for pre-monsoon was $0.661 > 0.6$ and for post-monsoon was $0.573 > 0.5$, and Bartlett's sphericity test significance $p < 0.05$ confirmed the suitability for PCA.

The factor analysis of hydrochemical species of groundwater resulted in six principal components (PC's) during the two seasons. The principal components contributed in 72.43 and 75.93% of total variance of hydrochemical dataset during pre- and post-monsoon season, respectively. The occurrence of hydrochemical species with higher loadings in a principal component suggests the common source or the associated vital process for the species (Houria et al. 2020). The rotated component matrix with factor loadings of each principal component for the hydrochemical parameters is shown in Table 7 and 8 for pre- and post-monsoon, respectively. The factor loadings can be designated as 'weak,' 'moderate' and 'strong,' for the absolute loading values of 0.50–0.30, 0.75–0.50 and > 0.75 , respectively (Liu et al. 2003).

The first factor or component has the highest eigenvector sum and represents the most important source of variation in hydrochemistry. Principal component-1 (PC1) accounts for 25.09 and 25.38% of the total variance and characterize water–rock interaction. PC1 represents the dominance

of loading by Cl^- , Mg, Ca, Na, EC and Sr with about 25% of total variance during both seasons. It shows the mineral (especially halite) dissolution and rock–water interaction as key processes within the study area. PC2 has a higher positive loading for CO_3^{2-} , HCO_3^- and SO_4^{2-} during pre-monsoon, whereas for CO_3^{2-} , HCO_3^- , pH, F^- during post-monsoon season. PC2 corresponds to augmentation of fluoride ion concentration in groundwater is due to slight alkaline medium supports silicate weathering and direct-ion exchange process. PC3 accounts for K, Mn, PO_4^{3-} during pre-monsoon and Cu, Fe and Be during post-monsoon, for higher positive loadings. PC4 explains the Be, F^- and pH during pre-monsoon and Zn, Mn during post-monsoon, for higher positive loadings. PC5 reveals the same source for Cu, Zn and Fe during pre-monsoon and SO_4^{2-} and K^+ during post-monsoon. PC6 explains NO_3^- during pre-monsoon and NO_3^- and PO_4^{3-} during post-monsoon, for higher positive loadings. The last factor or component shows the least important process contributing to the chemical variation.

Interpretation of hydrogeochemical processes controlling fluoride enrichment

The seasonal variation in groundwater quality parameters plotted on different scatter plots has revealed various hydrogeochemical processes dominant across both the basins. The processes are evaluated for the assessment of controlling factors in fluoride enrichment of groundwater. The scatter plot between Na^+ (meq/l) and Cl^- (meq/l) parameters has shown a quite close trendline to equiline with a higher R-squared (R^2) value. R^2 is also termed as the coefficient of determination and is a goodness-of-fit for linear regression model. Higher R^2 value explains smaller sum of squared residuals with a smaller difference between the observed data and the fitted value. The higher R^2 value during pre-monsoon (0.87) is shown in Fig. 6a1 and post-monsoon (0.82) is shown in Fig. 6a2. The scatter plots for both seasons have suggested that the equal concentrations of Na^+ and Cl^- in groundwater are resulted from the dissolution of halite minerals (Belkhir et al. 2011). The semiarid environment of the study area favors evaporation attributed to elevated concentrations of Na^+ and Cl^- in groundwater causing higher salinity (Fisher and Mullican 1997; Rena et al. 2021). So, the presence of halite minerals, weathering process and evaporation-induced higher ion concentration in groundwater of the study area account for higher salinity (Rao 2006). Moreover, the semiarid climate, long sunshine hours, hot summers and erratic rainfall play a crucial role in major groundwater character of Ruparail and Banganga basins.

The scatter plot for seasonal variation in between Na^+ / Cl^- and electrical conductivity (EC) during pre-monsoon and post-monsoon are shown in Fig. 6b1 and Fig. 6b2, respectively. The horizontal trendline for both the scatter

Table 7 Multivariate statistical analysis with factor loadings of significant principal components (eigenvalue > 1), eigenvalues, % of the variance and cumulative variance during pre-monsoon season

Hydrochemical parameter	Component					
	1	2	3	4	5	6
Cl ⁻	0.977	0.010	0.052	0.102	- 0.005	- 0.044
Mg	0.952	- 0.071	0.003	0.066	0.033	0.036
Ca	0.942	- 0.020	0.219	- 0.069	0.055	0.024
Na	0.915	0.245	0.063	0.212	- 0.009	- 0.049
EC	0.675	0.476	0.016	- 0.061	0.123	0.067
Sr	0.559	0.378	0.243	- 0.312	0.194	0.245
CO ₃ -2	0.032	0.859	- 0.055	0.015	0.054	- 0.095
HCO ₃ ⁻	- 0.034	0.829	- 0.030	0.327	- 0.042	- 0.058
SO ₄ -2	0.329	0.706	0.024	0.081	0.175	0.363
K	0.216	- 0.081	0.734	- 0.119	- 0.074	- 0.059
Mn	0.045	- 0.017	0.704	- 0.177	0.015	0.119
PO ₄ -3	- 0.037	0.116	0.506	0.459	0.229	0.171
Be	- 0.135	- 0.011	0.259	- 0.752	0.080	- 0.093
F ⁻	0.173	0.378	0.031	0.592	0.148	- 0.114
pH	- 0.386	0.192	- 0.201	0.481	- 0.071	- 0.340
Cu	- 0.038	0.144	- 0.039	0.042	0.766	- 0.124
Zn	0.035	- 0.094	- 0.315	- 0.210	0.621	0.471
Fe	0.229	0.028	0.356	0.092	0.569	- 0.021
NO ₃ ⁻	- 0.024	0.030	0.120	0.034	- 0.092	0.885
Eigen value	5.39	2.80	1.83	1.46	1.19	1.10
Total variance (%)	25.09	13.63	9.26	9.15	7.83	7.48
Cumulative variance (%)	25.09	38.72	47.98	57.12	64.95	72.43
Hydrogeologic process	Mineral (halite) dissolution and rock-water interaction	Silicate weathering and direct-ion exchange process	Synthetic fertilizer application	Evaporation and crystallization	Sorption process	Anthropogenic origin

plots shows the constant Na⁺/Cl⁻ ratio with the EC. The elevated values of EC confirm the higher salinity and the influence of evaporation and dissolution on the hydrochemistry of groundwater (Fisher and Mullican 1997). The elevated EC for both the basins during the post-monsoon season is suggestive of the leaching of minerals from aquifer sediments through weathering process caused by the infiltration of surface run-off water (Handa 1975; Rena et al. 2021; Singh et al. 2014).

The scatter plot for seasonal variation in between Cl⁻ + SO₄⁻² (mg/l) and Na⁺ + K⁺ (mg/l) is shown in Fig. 6c1 for pre-monsoon and Fig. 6c2 for post-monsoon seasons. The plots have revealed a quite close trendline to equiline with a higher value of R² as 0.90 during pre-monsoon and 0.85 during post-monsoon season. It explains that the samples having a higher concentration of (Na⁺ + K⁺) ions also have a higher concentration of (Cl⁻ + SO₄⁻²) ions in the groundwater regime. It confirms the common source and processes controlling the enrichment of these ions in the groundwater chemistry (Datta et al. 1996b; Rina et al. 2013). The ion exchange process is responsible for the exchange of

Na⁺ and K⁺ ions in the groundwater from Ca²⁺ and Mg²⁺ from host rock material and vice versa (Singh et al. 2013).

Chemical weathering plays a lead role in the dissolution of fluoride-bearing minerals governing by thermodynamic principles (Fuge 2018; Singh et al. 2018). For a better understanding of the dominant weathering process in the study area, a scatter plot between SO₄²⁻ + HCO₃⁻ (meq/l) and Ca²⁺ + Mg²⁺ (meq/l) is prepared for pre-monsoon in Fig. 6d1 and post-monsoon in Fig. 6d2. The scatter plot has suggested that the samples falling left to the equiline are having dominant carbonate weathering or reverse-ion exchange process. Except few samples, the samples falling right to the equiline are dominant with silicate weathering and direct-ion exchange process (Rina et al. 2013; Srinivasamoorthy et al. 2008). The evaluation of plots has resulted that the majority of the water samples having an excess of SO₄²⁻ + HCO₃⁻ concentration as compared to Ca²⁺ + Mg²⁺ concentration. It revealed the silicate weathering and direct-ion exchange processes as dominant processes across the study area (Cerling et al. 1989; Fisher

Table 8 Multivariate statistical analysis with factor loadings of significant principal components (Eigen value > 1), eigenvalues, % of the variance and cumulative variance during post-monsoon season

Hydrochemical parameter	Component					
	1	2	3	4	5	6
Cl ⁻	0.977	0.038	0.129	0.014	- 0.020	- 0.021
Mg	0.921	- 0.080	0.008	- 0.015	- 0.087	- 0.023
Na	0.882	0.302	0.135	0.002	0.098	- 0.011
Ca	0.866	- 0.153	0.103	0.296	0.073	0.091
EC (μS)	0.786	0.189	0.239	- 0.017	0.415	- 0.042
Sr	0.582	0.051	- 0.036	0.331	0.483	0.291
CO ₃ -2	- 0.003	0.907	0.048	- 0.108	0.070	0.064
HCO ₃ ⁻	0.076	0.895	0.048	- 0.097	0.141	0.091
pH	- 0.183	0.660	- 0.324	- 0.074	- 0.064	- 0.304
F ⁻	0.263	0.621	- 0.221	- 0.163	0.353	- 0.065
Cu	0.058	- 0.091	0.867	0.049	0.083	0.065
Fe	0.285	- 0.048	0.678	0.111	- 0.006	- 0.271
Be	0.015	- 0.230	- 0.054	0.799	- 0.103	0.128
Zn	0.147	- 0.112	0.181	0.663	0.212	- 0.313
Mn	0.061	0.022	0.454	0.594	- 0.323	0.204
SO ₄ -2	0.172	0.234	0.030	- 0.147	0.772	0.241
K	0.503	- 0.100	- 0.109	- 0.099	- 0.504	0.229
NO ₃ ⁻	- 0.097	- 0.340	0.100	- 0.059	0.121	0.725
PO ₄ -3	0.164	0.274	- 0.185	0.109	0.037	0.677
Eigen Value	5.29	3.55	1.69	1.57	1.26	1.07
Total variance (%)	25.38	15.47	9.34	9.18	8.50	8.07
Cumulative (%)	25.38	40.85	50.18	59.36	67.86	75.93
Hydrogeologic process	Mineral (halite) dissolution and rock-water interaction	Alkaline medium and silicate weathering, direct-ion exchange process	Sorption process	Sorption process	Synthetic fertilizers	Anthropogenic origin

and Mullican 1997). A few samples falling left to the equiline are suggestive of carbonate weathering process and reverse-ion exchange process (Datta et al. 1996a; Rajmohan and Elango 2004). Since silicate weathering favorably dissolves fluoride ions from aquifer material to groundwater, the fluoride enrichment is observed in the groundwater samples showing silicate weathering and direct-ion exchange process, whereas the inhibited fluoride ion concentration is found in the samples showing carbonate weathering and reverse-ion exchange process. (Jagadeshan et al. 2015; Singh et al. 2018).

In 1970, Gibbs has suggested a diagram between Na/(Na + Ca) and log TDS (mg/l) as a suitable method to identify conventional processes such as evaporation, rock dominance and precipitation controlling groundwater chemistry (Gibbs 1970). The Gibbs plot explains the water samples falling above the 1000 line of log TDS are suggestive of salinization induced by evaporation and crystallization processes, whereas the samples falling below 1000 line reveals the rock-dominant weathering process. The plot between

Na/(Na + Ca) and log TDS (mg/l) shown in Fig. 6e₁ for pre-monsoon and Fig. 6e₂ for post-monsoon, samples, has suggested that the evaporation and crystallization processes are responsible for rock-dominant weathering and salinization.

Geochemical modeling of mineral phases

Saturation index (SI) of a mineral phase reflects the thermodynamic tendency of the mineral to dissolve or precipitate in the solution. It is also useful to understand the origin of groundwater mineralization (Kumar et al. 2017). The geochemical modeling of mineral phase in a solution or groundwater is expressed as the SI-value. Based on the SI-value, the saturation states are termed as saturation (equilibrium, SI = 0), under-saturation (dissolution, SI < 0) and over-saturation (precipitation, SI > 0) states. The under-saturation reflects the insufficient amount of mineral in the solution or with short residence time of the mineral in the solution, whereas the over-saturation indicates the

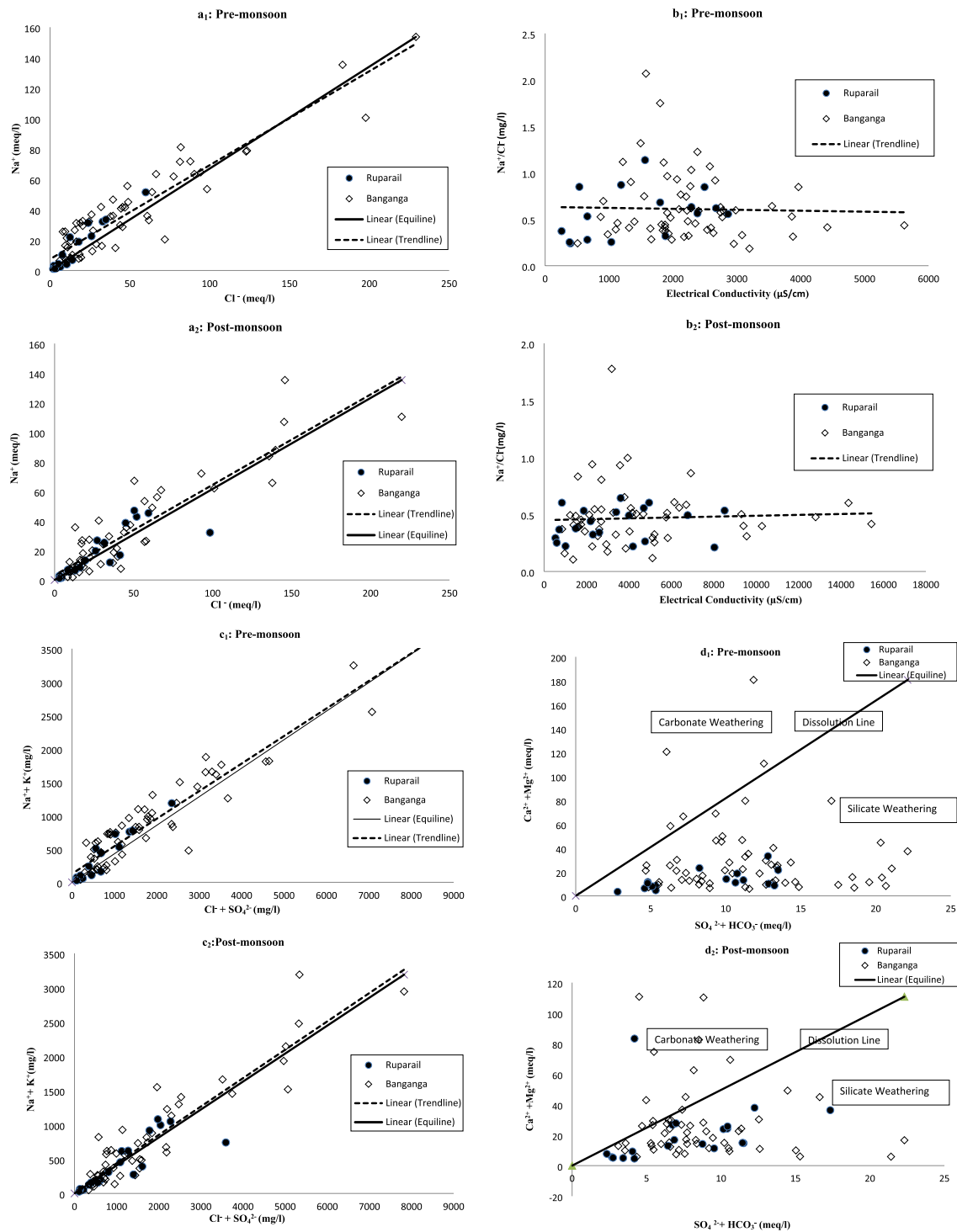


Fig. 6 Interpretation of various hydrogeological processes based on the scatter plots between Na⁺ (meq/l) and Cl⁻ (meq/l) for **a₁** Pre-monsoon and **a₂** Post-monsoon; between Na⁺/Cl⁻ (mg/l) and electrical conductivity (μS/cm) for **b₁** Pre-monsoon and **b₂** Post-monsoon; between Na⁺/(Na⁺+Ca²⁺) and log TDS (mg/l) (Gibbs' diagram) during **e₁** Pre-monsoon and **e₂** Post-monsoon seasons' groundwater samples

soon and **c₂** Post-monsoon; between SO₄²⁻+HCO₃⁻ (meq/l) and Ca²⁺+Mg²⁺ (meq/l) for **d₁** Pre-monsoon and **d₂** Post-monsoon and between Na⁺/(Na⁺+Ca²⁺) and log TDS (mg/l) (Gibbs' diagram) during **e₁** Pre-monsoon and **e₂** Post-monsoon seasons' groundwater samples

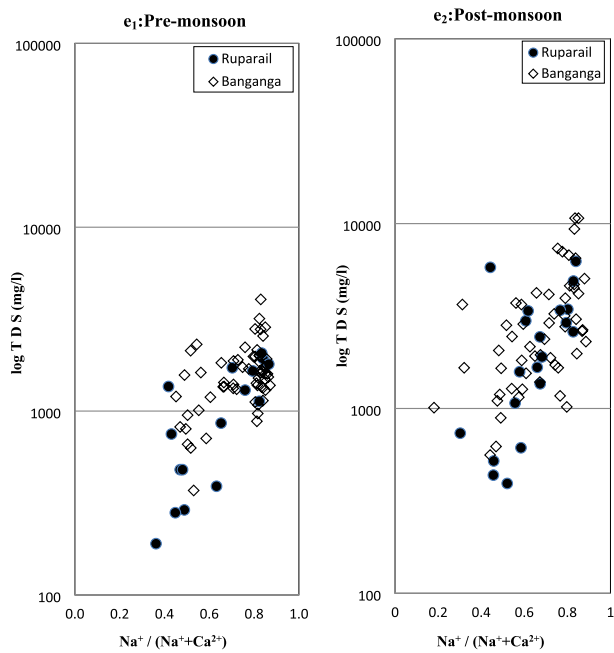


Fig. 6 (continued)

excessive amount of mineral in the solution or with long residence time to reach equilibrium. The under-saturation is expressed as a negative value showing a tendency to

dissolve, whereas the over-saturation is expressed as a positive value showing a tendency to precipitate from the groundwater of an aquifer.

The plots between SI-Calcite and SI-Fluorite for both the basins are shown in Fig. 7a1 for pre-monsoon and Fig. 7a2 for post-monsoon season within the study area. It has been observed that during both seasons and for both the basins, the majority of the water samples are over-saturated with calcite and under-saturated with fluorite. The under-saturation of fluorite mineral suggests that the mineral has a tendency to dissolve further and will cause fluoride enrichment in groundwater. The over-saturation of calcite indicates that high level of Ca^{2+} in groundwater might enhance the reverse-ion exchange process where Na^+ replaces Ca^{2+} on the surface of the rock matrices and release of Ca^{2+} in groundwater and evaporation in dry climate with aquifer matrices. So, the under-saturated fluorite mineral and over-saturated calcite mineral explain the precipitation of calcite (negative correlation) or carbonate minerals which are not responsible for such increase in fluoride ions in groundwater. The few samples showing saturation of fluorite mineral (equilibrium, $SI = 0$) are suggestive of a continual release of fluoride ions from the fluorite mineral in alkaline media. So, the varied values of mineral phases for the water samples control fluoride enrichment in groundwater chemistry.

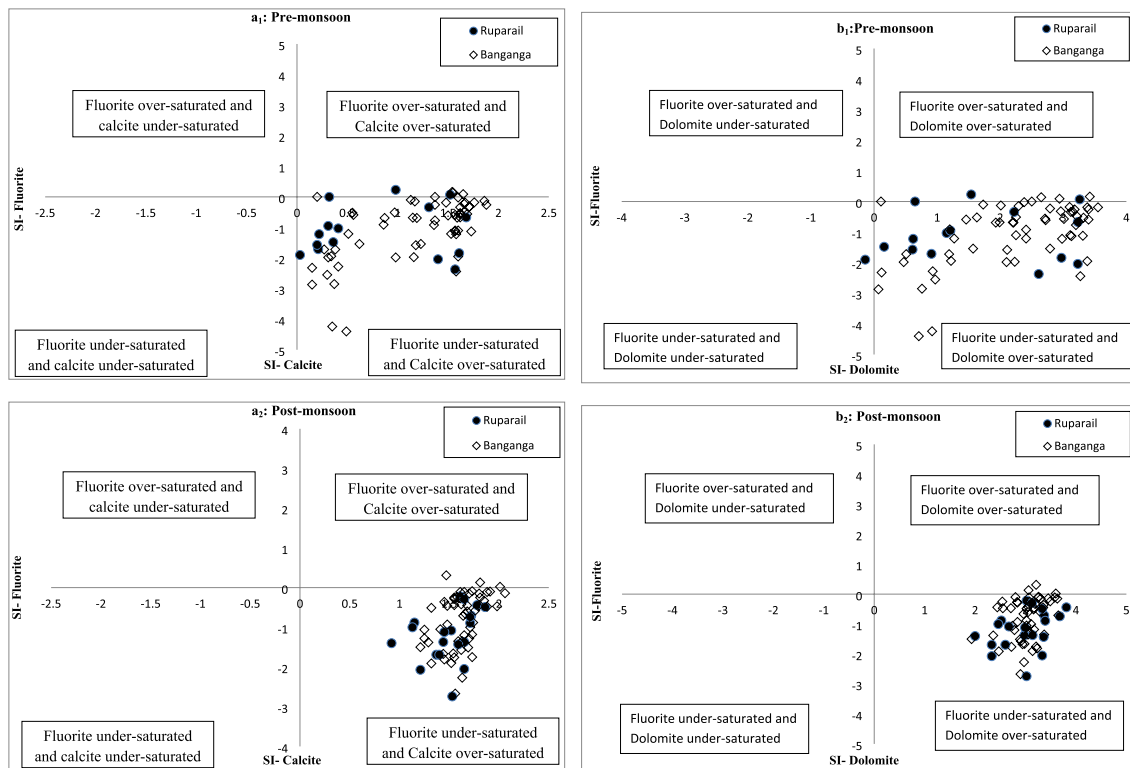


Fig. 7 Scatter plot between saturation index (SI)-Calcite and SI-Fluorite for a₁ Pre-monsoon and a₂ Post-monsoon groundwater samples and scatter plot between SI-Dolomite and SI-Fluorite for b₁ Pre-monsoon and b₂ Post-monsoon groundwater samples

The plots between SI-Dolomite and SI-Fluorite for both the basins are shown in Fig. 7b1 for pre-monsoon and Fig. 7b2 for post-monsoon season. The results have shown that the hydrochemistry of majority of the samples is over-saturated with dolomite and under-saturated with fluorite mineral during both seasons. The under-saturation of fluorite mineral has shown a tendency to dissolve further and supported the augmentation of fluoride ion concentration in groundwater. The over-saturation of dolomite depicted that the mineral dissolution is not responsible for elevated concentration of Mg^{2+} ions but the observed higher concentration is due to reverse-ion exchange process which also causes temporary hardness. Moreover, the under-saturation of fluorite and over-saturation of dolomite supports fluoride enrichment in groundwater of the study area. So, the state of mineral phases in the hydrochemistry plays a significant role in the augmentation or inhibition of fluoride ion concentration in groundwater of the study area.

Conclusions

The fluoride ion concentration in groundwater of Ruparail basins was found in the range of 0.09 mg/l to 3.80 mg/l (average 1.13 mg/l) during pre-monsoon, whereas it ranged from 0.11 mg/l to 2.12 mg/l (average 1.09 mg/l) during post-monsoon season. The groundwater of Banganga basin has resulted in the fluoride ion concentration ranging from 0.09 mg/l to 4.23 mg/l (average 1.37 mg/l) during pre-monsoon, whereas it ranged from 0.15 mg/l to 4.19 mg/l (average 1.50 mg/l) during post-monsoon season. The percentage of groundwater samples having fluoride ion concentration above the permissible limit of 1.5 mg/l as per WHO-2017 is found in 25 and 30% in Ruparail basin, whereas 41.67 and 50% in Banganga basin, during pre- and post-monsoon seasons, respectively. The hydrochemical analysis of groundwater samples for both the basins has resulted in a dominance of anions in the order of $Cl^- > HCO_3^- > SO_4^{-2} > NO_3^- > CO_3^{-2} > F^- > PO_4^{-3}$ and dominance of cations in the order of $Na^+ > Ca^{+2} > Mg^{+2} > K^+$ during both seasons. The Chadha plot of hydrochemical facies has revealed the water type of Na-Cl, followed by Ca-Mg-Cl in both the basins during pre-monsoon and in Banganga basin during post-monsoon season only. The groundwater samples of Ruparail basin during post-monsoon have resulted in the water type of Ca-Mg-Cl, followed by Na-Cl type. The Na-Cl water type is shows greater salinity hazard and dominant silicate weathering process responsible for fluoride enrichment of groundwater, whereas the Ca-Mg-Cl water type is having permanent hardness and reverse-ion exchange process responsible for inhibited fluoride ion concentration. The interpretation of hydrogeochemical processes based on the scatter plots of

various hydrochemical parameters has revealed the silicate weathering, direct-ion exchange, mineral dissolution, crystallization, salinization, rock-water interaction and evaporation processes responsible for fluoride enrichment of groundwater. The inhibited fluoride ion concentration is attributed to carbonate weathering and reverse-ion exchange processes. The geochemical modeling of thermodynamic nature of various mineral phases in groundwater explains over-saturation of calcite and dolomite with under-saturation of fluorite, supporting augmentation of fluoride in groundwater. The semiarid climate, lack of recharge due to erratic rainfall and overdraft of groundwater support the dissolution of fluoride-bearing minerals from the aquifer material and leaching into groundwater. The comprehensive understanding of hydrogeochemical processes controlling fluoride ion concentration in groundwater is of great use for planning strategies adopted for water resource management for drinking purposes in a sustained way.

Acknowledgements The authors are grateful to the Indian Space Research Organisation (ISRO), India, for providing 'Bhuvan' web-based GIS tool, Geological Survey of India (GSI) for providing geoscientific information through 'Bhukosh' gateway, National Aeronautics and Space Administration (NASA, USA) for providing digital elevation data (SRTM-30 m) and Planet labs for satellite data (RapidEye 2) of the study area. The authors would also like to extend thanks to University Grants Commission (UGC) for providing financial support for this research in the form of fellowship grants. The authors are also pleased to acknowledge Central Instrumentation Facility (CIF) at the School of Environmental Sciences, Jawaharlal Nehru University, for providing AAS and ICP-OES facility. The authors also duly acknowledge to the editor and anonymous reviewers of the journal for their worth full suggestions and comments which significantly helped to improve the manuscript.

Funding Not applicable.

Availability of data and material Not applicable.

Code availability Not applicable.

Declarations

Conflict of interest The authors declare that they have no known competing financial interests or personal relationships that could have appeared to influence the work reported in this paper.

References

- Adams S, Titus R, Pietersen K, Tredoux G, Harris C (2001) Hydrochemical characteristics of aquifers near Sutherland in the Western Karoo, South Africa. *J Hydrol* 241:91–103. [https://doi.org/10.1016/S0022-1694\(00\)00370-X](https://doi.org/10.1016/S0022-1694(00)00370-X)
- Adimalla N (2020) Assessment and mechanism of fluoride enrichment in groundwater from the hard rock terrain: a multivariate

- statistical approach. *Geochem Int* 58:456–471. <https://doi.org/10.1134/S0016702920040060>
- Adimalla N, Li P, Qian H (2018) Evaluation of groundwater contamination for fluoride and nitrate in semi-arid region of Nirmal Province, South India: a special emphasis on human health risk assessment (HHRA). *Hum Ecol Risk Assess Int J*. <https://doi.org/10.1080/10807039.2018.1460579>
- Adimalla N, Marsetty SK, Xu P (2020) Assessing groundwater quality and health risks of fluoride pollution in the Shasler Vagu (SV) watershed of Nalgonda, India. *Hum Ecol Risk Assess Int J* 26:1569–1588. <https://doi.org/10.1080/10807039.2019.1594154>
- Adimalla N, Qian H, Nandan M (2020) Groundwater chemistry integrating the pollution index of groundwater and evaluation of potential human health risk: a case study from hard rock terrain of south India. *Ecotoxicol Environ Saf* 206:111217. <https://doi.org/10.1016/j.ecoenv.2020.111217>
- Adimalla N, Qian H, Tiwari DM (2021) Groundwater chemistry, distribution and potential health risk appraisal of nitrate enriched groundwater: a case study from the semi-urban region of South India. *Ecotoxicol Environ Saf* 207:111277. <https://doi.org/10.1016/j.ecoenv.2020.111277>
- Agrawal V, Vaish A, Vaish P (1997) Groundwater quality: focus on fluoride and fluorosis in Rajasthan. *Curr Sci* 73:743–746. <https://www.jstor.org/stable/24100412>
- Association APH (1995) Standard methods for the examination of water and wastewater. American public health association, Washington DC
- Athavale R, Das R (1999) Beware! fluorosis is zeroing in on you. *Down Earth* 8:24–25
- Ayoob S, Gupta AK (2006) Fluoride in drinking water: a review on the status and stress effects. *Crit Rev Environ Sci Technol* 36:433–487. <https://doi.org/10.1080/10643380600678112>
- Bandyopadhyay S, Srivastava S, Jha MK, Hegde V, Jayaraman V (2007) Harnessing earth observation (EO) capabilities in hydrogeology: an Indian perspective. *Hydrogeol J* 15:155–158. <https://doi.org/10.1007/s10040-006-0122-4>
- Belkhir L, Boudoukha A, Mouni L (2011) A multivariate statistical analysis of groundwater chemistry data. *Int J Environ Res (IJER)* 5(2):537–544. <https://www.sid.ir/en/journal/ViewPaper.aspx?id=195027>
- Bo Z, Mei H, Yongsheng Z, Xueyu L, Xuelin Z, Jun D (2003) Distribution and risk assessment of fluoride in drinking water in the west plain region of Jilin province, China. *Environ Geochem Health* 25:421–431. <https://doi.org/10.1023/B:EGAH.000004560.47697.91>
- Boyle D, Chagnon M (1995) An incidence of skeletal fluorosis associated with groundwaters of the maritime carboniferous basin, Gaspé region, Quebec, Canada. *Environ Geochem Health* 17:5–12. <https://doi.org/10.1007/BF00188625>
- Bureau of Indian Standards (2015) Indian Standard, DRINKING WATER — SPECIFICATION (Second Revision). Amendment Number 1 June 2015 to IS 10500: 2012, Drinking Water-Specification
- Cattell RB, Jaspers J (1967) A general plasmode (No. 30-10-5-2) for factor analytic exercises and research. *Multivariate Behav Res Monogr* 67-3:211. <https://psycnet.apa.org/record/1968-09684-001>
- Cerling T, Pederson B, Von Damm K (1989) Sodium-calcium ion exchange in the weathering of shales: Implications for global weathering budgets. *Geology* 17:552–554. [https://doi.org/10.1130/0091-7613\(1989\)017%3c0552:SCIEIT%3e2.3.CO;2](https://doi.org/10.1130/0091-7613(1989)017%3c0552:SCIEIT%3e2.3.CO;2)
- CGWB (2017) Report on aquifer mapping and ground water management district Bharatpur, rajasthan (under XII plan) Central Ground Water Board Ministry of Water Resources. River Development & Ganga Rejuvenation Government of India Western Region, Jaipur
- Chadha D (1999) A proposed new diagram for geochemical classification of natural waters and interpretation of chemical data. *Hydrogeol J* 7:431–439. <https://doi.org/10.1007/s100400050216>
- Chadha DK (2006) Development of an integrated spatial data base for sustainable ground water management plan Bharatpur district Rajasthan. Department of Science and Technology Government of India, New Delhi
- Chouhan S, Flora S (2010) Arsenic and fluoride: two major ground water pollutants. <http://nopr.niscair.res.in/handle/123456789/9735>
- Cotruvo JA (2017) WHO guidelines for drinking water quality: first addendum to the. *J-Amer Water Work Assoc* 109:44–51. <https://doi.org/10.5942/jawwa.2017.109.0087>
- Datta P, Bhattacharya S, Tyagi S (1996) 18O studies on recharge of phreatic aquifers and groundwater flow-paths of mixing in the Delhi area. *J Hydrol* 176:25–36. [https://doi.org/10.1016/0022-1694\(95\)02784-X](https://doi.org/10.1016/0022-1694(95)02784-X)
- Datta P, Deb D, Tyagi S (1996) Stable isotope (18O) investigations on the processes controlling fluoride contamination of groundwater. *J Contam Hydrol* 24:85–96. [https://doi.org/10.1016/0169-7722\(96\)00004-6](https://doi.org/10.1016/0169-7722(96)00004-6)
- Diatloff E, Rengel Z (2001) Compilation of simple spectrophotometric techniques for the determination of elements in nutrient solutions. *J Plant Nutr* 24:75–86. <https://doi.org/10.1081/PLN-100000313>
- Din SU, Javed A (1997) Geomorphology and landscape evolution of bharatpur district, rajasthan. *J Indian Soc Remote Sens* 25:177. <https://doi.org/10.1007/BF03024219>
- Dubey HV, Ingle NA, Gupta R, Charania Z, Ingle E, Sharma I (2015) Prevalence of dental fluorosis among 12–15 years school children of Bharatpur city: a cross-sectional study. *J Indian Assoc Pub Health Dent* 13:405
- Elango L, Ramachandran S, Chowdary YN (1992) Groundwater quality in coastal regions of South Madras. *Indian J Environ Health* 34:318–325
- Fazelabdolabadi B, Golestan MH (2020) Towards Bayesian quantification of permeability in micro-scale porous structures—the database of micro networks. *HighTech Innov J* 1:148–160. <https://doi.org/10.28991/HIJ-2020-01-04-02>
- Fisher RS, Mullican WF III (1997) Hydrochemical evolution of sodium-sulfate and sodium-chloride groundwater beneath the northern Chihuahuan Desert, Trans-Pecos, Texas, USA. *Hydrogeol J* 5:4–16. <https://doi.org/10.1007/s100400050102>
- Fuge R (2018) Fluorine in the environment, a review of its sources and geochemistry. *Appl Geochem*. <https://doi.org/10.1016/j.apgeochem.2018.12.016>
- Ga NRSC (2012) National geomorphological and lineament mapping on 1:50,000 scale. National Remote Sensing Centre, ISRO, Hyderabad
- Gibbs RJ (1970) Mechanisms controlling world water chemistry. *Science* 170:1088–1090. <https://doi.org/10.1126/science.170.3962.1088>
- Handa B (1975) Geochemistry and genesis of fluoride-containing ground waters in India. *Groundwater* 13:275–281. <https://doi.org/10.1111/j.1745-6584.1975.tb03086.x>
- Houria B, Mahdi K, Zohra TF (2020) Hydrochemical characterisation of groundwater quality: Merdja plain (Tebessa town, Algeria). *Civil Eng J* 6:318–325. <https://doi.org/10.28991/cej-2020-03091473>
- Hussain MR, Abed BS (2019) Simulation and assessment of groundwater for domestic and irrigation uses. *Civil Eng J* 5:1877–1892. <https://doi.org/10.28991/cej-2019-03091379>
- Hussain J, Hussain I, Sharma K (2010) Fluoride and health hazards: community perception in a fluorotic area of central Rajasthan (India): an arid environment. *Environ Monit Assess* 162:1–14. <https://doi.org/10.1007/s10661-009-0771-6>

- Hussain I, Arif M, Hussain J (2012) Fluoride contamination in drinking water in rural habitations of Central Rajasthan, India. *Environ Monit Assess* 184:5151–5158. <https://doi.org/10.1007/s10661-011-2329-7>
- Jagadeshan G, Kalpana L, Elango L (2015) Hydrogeochemistry of high fluoride groundwater in hard rock aquifer in a part of Dharmapuri district, Tamil Nadu, India. *Geochem Int* 53:554–564. <https://doi.org/10.1134/S0016702915060038>
- Jin C, Yan Z, Jianwei L, Ruodeng X, Sangbu D (2000) Environmental fluoride content in Tibet. *Environ Res* 83:333–337. <https://doi.org/10.1006/enrs.2000.4066>
- Kaiser HF (1960) The application of electronic computers to factor analysis. *Educ Psychol Measur* 20:141–151. <https://doi.org/10.1177/001316446002000116>
- Kharb P, Susheela A (1994) Fluoride ingestion in excess and its effect on organic and certain inorganic constituents of soft tissues. *Med Sci Res* 22:43–44
- Kumar PS, Jegathambal P, James E (2011) Multivariate and geostatistical analysis of groundwater quality in Palar river basin. *Int J Geol* 4:108–119
- Kumar PS, Elango L, James E (2014) Assessment of hydrochemistry and groundwater quality in the coastal area of South Chennai, India. *Arab J Geosci* 7:2641–2653. <https://doi.org/10.1007/s12517-013-0940-3>
- Kumar P, Singh CK, Saraswat C, Mishra B, Sharma T (2017) Evaluation of aqueous geochemistry of fluoride enriched groundwater: a case study of the Patan district, Gujarat, Western India. *Water Science* 31:215–229. <https://doi.org/10.1016/j.wsj.2017.05.002>
- Liu C-W, Lin K-H, Kuo Y-M (2003) Application of factor analysis in the assessment of groundwater quality in a blackfoot disease area in Taiwan. *Sci Total Environ* 313:77–89. [https://doi.org/10.1016/S0048-9697\(02\)00683-6](https://doi.org/10.1016/S0048-9697(02)00683-6)
- Maheshwari R (2006) Fluoride in drinking water and its removal. *J Hazard Mater* 137:456–463. <https://doi.org/10.1016/j.jhazmat.2006.02.024>
- Mohammadi Z (2009) Assessing hydrochemical evolution of groundwater in limestone terrain via principal component analysis. *Environ Earth Sci* 59:429–439. <https://doi.org/10.1007/s12665-009-0041-5>
- Mohapatra P, Vijay R, Pujari P, Sundaray S, Mohanty B (2011) Determination of processes affecting groundwater quality in the coastal aquifer beneath Puri city, India: a multivariate statistical approach. *Water Sci Technol* 64:809–817. <https://doi.org/10.2166/wst.2011.605>
- Mondal D, Gupta S, Reddy D, Nagabhushanam P (2014) Geochemical controls on fluoride concentrations in groundwater from alluvial aquifers of the Birbhum district, West Bengal, India. *J Geochem Explor* 145:190–206. <https://doi.org/10.1016/j.gexplo.2014.06.005>
- Mondal N, Tiwari K, Sharma K, Ahmed S (2016) A diagnosis of groundwater quality from a semiarid region in Rajasthan, India. *Arab J of Geosci* 9:602. <https://doi.org/10.1007/s12517-016-2619-z>
- Muralidharan D, Nair AP, Sathyanarayana U (2002) Fluoride in shallow aquifers in Rajgarh Tehsil of Churu District, Rajasthan—an arid environment. *Curr Sci* 83:699–702. <https://www.jstor.org/stable/24106144>
- Priscoli JD (2000) Water and civilization: using history to reframe water policy debates and to build a new ecological realism. *Water Policy* 1:623–636. [https://doi.org/10.1016/S1366-7017\(99\)00019-7](https://doi.org/10.1016/S1366-7017(99)00019-7)
- Rajmohan N, Elango L (2004) Identification and evolution of hydrogeochemical processes in the groundwater environment in an area of the Palar and Cheyyar River Basins, Southern India. *Environ Geol* 46:47–61. <https://doi.org/10.1007/s00254-004-1012-5>
- Raju NJ, Dey S, Das K (2009) Fluoride contamination in groundwaters of Sonbhadra District, Uttar Pradesh, India. *Current Science* 96:979–985. <https://www.jstor.org/stable/24104691>
- Rao NS (2006) Seasonal variation of groundwater quality in a part of Guntur District, Andhra Pradesh, India. *Environ Geol* 49:413–429. <https://doi.org/10.1007/s00254-005-0089-9>
- Ravikumar P, Somashekar R (2017) Principal component analysis and hydrochemical facies characterization to evaluate groundwater quality in Varahi river basin, Karnataka state, India. *Appl Water Sci* 7:745–755. <https://doi.org/10.1007/s13201-015-0287-x>
- Rena V, Kamal V, Singh D, Roy N, Shikha A, Mukherjee S (2021) Hydrogeological assessment of high salinity in groundwater in parts of Bharatpur district, Rajasthan, India. *Eco Environ Cons* 27:S372–S380. <http://www.envirobiotechjournals.com/EECV27maysuppli2021/EECV-52.pdf>
- Rina K, Singh CK, Datta P, Singh N, Mukherjee S (2013) Geochemical modelling, ionic ratio and GIS based mapping of groundwater salinity and assessment of governing processes in Northern Gujarat, India. *Environ Earth Sci* 69:2377–2391. <https://doi.org/10.1007/s12665-012-2067-3>
- Salifu A, Petrushevski B, Ghebremichael K, Buamah R, Amy G (2012) Multivariate statistical analysis for fluoride occurrence in groundwater in the Northern region of Ghana. *J Contam Hydrol* 140:34–44. <https://doi.org/10.1016/j.jconhyd.2012.08.002>
- Saxena S, Saxena U (2013) Study of fluoride contamination status of ground water in Bassi Tehsil of district Jaipur, Rajasthan, India. *Int J Environ Sci* 3:2251–2260. <https://doi.org/10.6088/ijes.2013030600040>
- Singh P, Rani B, Singh U, Maheshwari R (2011) Fluoride contamination in ground water of Rajasthan and its mitigation strategies. *J pharmaceutical Bio-med Sci* 6(6):1–12
- Singh B, Gaur S, Garg V (2007) Fluoride in drinking water and human urine in Southern Haryana, India. *J Hazard Mater* 144:147–151. <https://doi.org/10.1016/j.jhazmat.2006.10.010>
- Singh CK, Rina K, Singh R, Shashtri S, Kamal V, Mukherjee S (2011) Geochemical modeling of high fluoride concentration in groundwater of Pokhran area of Rajasthan, India. *Bull Environ Contam Toxicol* 86:152–158. <https://doi.org/10.1007/s00128-011-0192-4>
- Singh CK, Kumari R, Singh N, Mallick J, Mukherjee S (2013) Fluoride enrichment in aquifers of the Thar Desert: controlling factors and its geochemical modelling. *Hydrol Process* 27:2462–2474. <https://doi.org/10.1002/hyp.9247>
- Singh N, Singh RP, Mukherjee S, McDonald K, Reddy K (2014) Hydrogeological processes controlling the release of arsenic in parts of 24 Parganas district, West Bengal. *Environ Earth Sci* 72:111–118. <https://doi.org/10.1007/s12665-013-2940-8>
- Singh P, Asthana H, Rena V, Kumar P, Kushawaha J, Mukherjee S (2018) Hydrogeochemical processes controlling fluoride enrichment within alluvial and hard rock aquifers in a part of a semi-arid region of Northern India. *Environ Earth Sci* 77:475. <https://doi.org/10.1007/s12665-018-7656-3>
- Srinivasamoorthy K, Chidambaram S, Prasanna M, Vasanthavihar M, Peter J, Anandhan P (2008) Identification of major sources controlling groundwater chemistry from a hard rock terrain—A case study from Mettur taluk, Salem district, Tamil Nadu. *India J Earth Syst Sci* 117:49. <https://doi.org/10.1007/s12040-008-0012-3>
- Subba Rao N, Sunitha B, Adimalla N, Chaudhary M (2020) Quality criteria for groundwater use from a rural part of Wanaparthy district, Telangana State, India, through ionic spatial distribution (ISD), entropy water quality index (EWQI) and principal component analysis (PCA). *Environ Geochem Health* 42:579–599. <https://doi.org/10.1007/s10653-019-00393-5>
- Subramani T, Elango L, Damodarasamy S (2005) Groundwater quality and its suitability for drinking and agricultural use in Chithar River Basin, Tamil Nadu, India. *Environ Geol* 47:1099–1110. <https://doi.org/10.1007/s00254-005-1243-0>

- Susheela A (1999) Fluorosis management programme in India. *Curr Sci* 77:1250–1256. <https://www.jstor.org/stable/24104407>
- Thanh NT (2019) Evaluation of multi-precipitation products for multi-time scales and spatial distribution during 2007–2015. *Civil Eng J* 5:255–267. <https://doi.org/10.28991/cej-2019-03091242>
- Tiwari K, Mondal N (2018) Hydrochemical characteristics of groundwater in Mahua Block, Dausa District, Rajasthan with a special reference to fluoride concentration. *J Himalayan Ecol Sustain Dev*. <https://doi.org/10.1080/02508069208686135>
- Vikas C, Kushwaha R, Ahmad W, Prasannakumar V, Reghunath R (2013) Genesis and geochemistry of high fluoride bearing groundwater from a semi-arid terrain of NW India. *Environ Earth Sci* 68:289–305. <https://doi.org/10.1007/s12665-012-1739-3>
- Vyas SK, Sharma G, Mathur Y, Chandwani V (2016) Interlinking feasibility of five river basins of Rajasthan in India. *Perspect Sci* 8:83–86. <https://doi.org/10.1016/j.pisc.2016.04.002>
- World Health Organization (2017) Guidelines for drinking-water quality: fourth edition incorporating the first addendum. Licence: CC BY-NC-SA 3.0 IGO. ISBN 978-92-4-154995-0
- Yadav MS, Kanga S, Singh SK (2019) Groundwater prospect zonation using frequency ratio model for Banganga River Basin, India. *Int J Eng Adv Technol (IJEAT)*. <https://doi.org/10.35940/ijeat.F8019.088619>
- Yevjevich V (1992) Water and Civilization. *Water Int* 17:163–171. <https://doi.org/10.1080/02508069208686135>
- Zaidi FK, Nazzal Y, Jafri MK, Naeem M, Ahmed I (2015) Reverse ion exchange as a major process controlling the groundwater chemistry in an arid environment: a case study from northwestern Saudi Arabia. *Environ Monit Assess* 187:607. <https://doi.org/10.1007/s10661-015-4828-4>
- Zandi S, Ghobakhlou A, Sallis P (2011) Evaluation of spatial interpolation techniques for mapping soil pH. International Congress on Modelling and Simulation (MODSIM 2011), Perth, Australia. Modelling and Simulation Society of Australia and New Zealand <http://www.mssanz.org.au/modsim2011>. 2011-12-12–2011-12-16, pp 1153–1159. <https://doi.org/10.1007/s10661-015-4828-4>

Publisher's Note Springer Nature remains neutral with regard to jurisdictional claims in published maps and institutional affiliations.

Springer Nature or its licensor holds exclusive rights to this article under a publishing agreement with the author(s) or other rightsholder(s); author self-archiving of the accepted manuscript version of this article is solely governed by the terms of such publishing agreement and applicable law.